

1 **Combination of novel and public RNA-seq datasets to generate an mRNA expression atlas for**  
2 **the domestic chicken**

3  
4 Stephen J. Bush<sup>1</sup>, Lucy Freem<sup>1</sup>, Amanda J. MacCallum<sup>1</sup>, Jenny O'Dell<sup>1, 2</sup>, Chunlei Wu<sup>3</sup>, Cyrus  
5 Afrasiabi<sup>3</sup>, Androniki Psifidi<sup>1, 4</sup>, Mark P. Stevens<sup>1</sup>, Jacqueline Smith<sup>1</sup>, Kim M. Summers<sup>1, 5</sup>, David A.  
6 Hume<sup>1, 5 \*</sup>

7  
8 <sup>1</sup> The Roslin Institute, University of Edinburgh, Easter Bush Campus, Edinburgh, Midlothian,  
9 EH25 9RG, UK

10 <sup>2</sup> Current address: Rivers and Lochs Institute, Inverness College, University of the Highlands  
11 and Islands, Research Hub, 1 Inverness Campus, Inverness, IV2 5NA, UK

12 <sup>3</sup> Department of Integrative and Computational Biology, The Scripps Research Institute,  
13 10550 North Torrey Pines Road, La Jolla, CA 92037, USA

14 <sup>4</sup> Current address: The Royal Veterinary College, Hawkshead Lane, Hatfield, Hertfordshire,  
15 AL9 7TA, UK

16 <sup>5</sup> Current address: Mater Research-University of Queensland, Translational Research  
17 Institute, 37 Kent Street, Woolloongabba, Queensland 4102, Australia

18 \*Corresponding author: [david.hume@uq.edu.au](mailto:david.hume@uq.edu.au), [david.hume@roslin.ed.ac.uk](mailto:david.hume@roslin.ed.ac.uk)

19  
20 Email addresses:  
21 Stephen J. Bush [stephen.bush@roslin.ed.ac.uk](mailto:stephen.bush@roslin.ed.ac.uk)  
22 Lucy Freem [lucy.freem@roslin.ed.ac.uk](mailto:lucy.freem@roslin.ed.ac.uk)

23	Amanda J. MacCallum	amanda.maccallum@roslin.ed.ac.uk
24	Jenny O'Dell	jenny.odell.ic@uhi.ac.uk
25	Chunlei Wu	cwu@scripps.edu
26	Cyrus Afrasiabi	cyrus@scripps.edu
27	Androniki Psifidi	apsifidi@rvc.ac.uk
28	Mark P. Stevens	mark.stevens@roslin.ed.ac.uk
29	Jacqueline Smith	jacqueline.smith@roslin.ed.ac.uk
30	Kim M. Summers	kim.summers@roslin.ed.ac.uk
31	David A. Hume	david.hume@uq.edu.au, david.hume@roslin.ed.ac.uk
32		

33 **ABSTRACT**

34 **Background**

35 The domestic chicken (*Gallus gallus*) is widely used as a model in developmental biology and is also  
36 an important livestock species. We describe a novel approach to data integration to generate an mRNA  
37 expression atlas for the chicken spanning major tissue types and developmental stages, using a diverse  
38 range of publicly-archived RNA-seq datasets and new data derived from immune cells and tissues.

39

40 **Results**

41 Randomly down-sampling RNA-seq datasets to a common depth and quantifying expression against a  
42 reference transcriptome using the mRNA quantitation tool Kallisto ensured that disparate datasets  
43 explored comparable transcriptomic space. The network analysis tool Miru was used to extract clusters  
44 of co-expressed genes from the resulting expression atlas, many of which were tissue or cell-type  
45 restricted, contained transcription factors that have previously been implicated in their regulation, or  
46 were otherwise associated with biological processes, such as the cell cycle. The atlas provides a  
47 resource for the functional annotation of genes that currently have only a locus ID. We cross-  
48 referenced the RNA-seq atlas to a publicly available embryonic Cap Analysis of Gene Expression  
49 (CAGE) dataset to infer the developmental time course of organ systems, and to identify a signature of  
50 the expansion of tissue macrophage populations during development.

51

52 **Conclusion**

53 Expression profiles obtained from public RNA-seq datasets – despite being generated by  
54 different laboratories using different methodologies – can be made comparable to each other.  
55 This meta-analytic approach to RNA-seq can be extended with new datasets from novel  
56 tissues, and is applicable to any species.

57

58 **INTRODUCTION**

59 Aggregation and meta-analysis of multiple large gene expression datasets based upon common  
60 microarray platforms is relatively commonplace in many species (e.g. [1-3]). Although RNA-seq is  
61 rapidly supplanting microarrays for gene expression profiling, it is not yet clear whether data from  
62 multiple different labs can be analysed together in an informative manner. Confounding variables  
63 reflect the many technical – and bias-prone – aspects of library preparation and sequencing (see  
64 reviews [4, 5]), with RNA-seq datasets often differing in read length [6], depth of coverage [7], strand  
65 specificity [8], RNA extraction and library selection methods [9], sequencing platform [10, 11] and the  
66 choice to sequence single- or paired-end reads [12]. For a given dataset, these variables can together  
67 affect both the number and type of genes detectable and the accuracy of their expression level  
68 estimates. Expression quantification is also affected by sample quality [13] and storage method [14],  
69 irrespective of sequencing technique: RNA degrades with lengthier post-mortem intervals [15] (the  
70 extent of which is tissue-dependent [16]) with degradation resulting in inaccurate quantification,  
71 particularly for shorter transcripts [17]. Sequencing composite biological structures (those with  
72 internal structures that have distinct functions), whether intentionally or inadvertently, can mask the  
73 signal of structure-specific differential expression [18]. Despite these variables, meta-analysis  
74 combining mammalian gene expression datasets [19-21] suggests that RNA-seq datasets are generally  
75 robust to inter-study variation, with the expression profiles of homologous tissues clustering more  
76 closely with each other than with different samples from the same study or species [22].  
77 Expression atlases are valuable resources for functional genomics. Groups of transcripts – members of  
78 which will have similar expression profiles – can be associated with a shared function, such as a  
79 particular pathway or biological process. This principle is known as ‘guilt by association’ [23] and has  
80 previously been used to annotate genes of unknown function in human [2, 24, 25], pig [26], sheep [27]  
81 and mouse [28, 29] datasets. Co-expression information is also informative in genome-wide  
82 association studies (GWAS) of complex traits and disease susceptibility. The simple principle, that

83 genes involved in the same trait or phenotype tend to be expressed in the same cell type or tissue, or  
84 otherwise participate in the same pathway, has been confirmed in multiple datasets [28, 30].  
85 Because of the ease of access *in ovo*, the chicken (*Gallus gallus*) embryo has been widely used as a  
86 model system in cell and developmental biology, constrained only by methods for genomic  
87 manipulation *in situ*, or in the germ line. These constraints were largely overcome through the  
88 sequencing of the genome, and technological developments such as *in vivo* electroporation, more  
89 than 15 years ago [31, 32]. More recent innovations including the generation of reporter transgenes  
90 [33] and genome editing via primordial germ cells [34-36] have transformed the utility of the  
91 chicken as a model organism. However, the current genome build still has many unannotated or  
92 minimally annotated genes about which very little is known [28]. Of the 18,347 protein-coding  
93 genes in version GalGal5 of the chicken genome in Ensembl89, 7275 (40%) have only been  
94 assigned an Ensembl placeholder ID.  
95 The domestic chicken is also a major source of animal protein worldwide, with different lines  
96 heavily selected for optimal production traits such as increased egg production or rapid  
97 weight gain. The molecular basis for these traits is increasingly being associated with  
98 genomic loci through genome-wide association studies based upon high density SNP  
99 platforms [37]. Both the application of the chick as a model organism, and for candidate gene  
100 analysis in genomic intervals associated with trait variation, would be expedited by  
101 improvements in functional genome annotation. In particular, it would be useful to identify  
102 the sets of protein-coding genes that share transcriptional regulation between the chick and  
103 the mouse, the most widely-studied mammalian model organism. For this purpose, we aimed  
104 to generate a comprehensive atlas of mRNA expression for the chicken.  
105 With the removal of antibiotics from the food chain and threats from emerging diseases, there is  
106 also interest in the selection of birds with increased disease resistance and/or resilience [38]. To  
107 support this activity, we were particularly interested in identifying and annotating genes expressed

108 specifically at high levels in cells of the innate immune system. Such gene sets have been identified  
109 in previous studies of human [2, 24, 25], pig [26], sheep [27] and mouse [28].  
110 The current version of the chicken assembly was largely derived from high-throughput (i.e.  
111 comparatively cheap but imprecise) short read sequencing and primarily contains protein-coding  
112 gene models. The recent use of long-read – PacBio SMRT Iso-Seq – data has demonstrated that the  
113 transcriptomic complexity of chickens is comparable to humans, with many additional lncRNA  
114 models (among others) scheduled for inclusion in future Ensembl annotations [39].  
115 To identify the set of genes expressed in innate immune cells in both unchallenged and activated  
116 conditions, we generated pure cultures of bone marrow-derived macrophages (BMDMs) grown in the  
117 presence of recombinant chicken macrophage colony-stimulating factor (CSF1), and stimulated them  
118 with the archetypal microbial agonist, lipopolysaccharide (LPS) [40]. To complement the data  
119 generated from macrophages *in vitro*, we also obtained RNA-seq libraries from the caecal tonsils of  
120 birds infected with *Campylobacter*, as well as from previous studies of macrophage, dendritic cell and  
121 heterophil populations. A global expression atlas for the chicken transcriptome was created by  
122 combining our immune-related data with 20 publicly archived RNA-seq datasets. Some were collated  
123 by the Avian RNA-seq Consortium [41], while others are drawn from a diverse range of existing  
124 publications, including studies that characterised the genetic basis of retinogenesis [42], the genetic  
125 determinants of meat tenderness [43], the morphological diversity of skin appendages [44], visceral fat  
126 metabolism [45], the transition between laying and brooding phases [46], the effect of heat stress upon  
127 pituitary development [47] and spleen function [48], the pathways involved in avian influenza  
128 resistance [49], the role of lncRNAs in the development of muscle [50], liver and adipose [51], and the  
129 transcriptional landscape of mRNA editing [52]. In total, 279 RNA-seq libraries were obtained,  
130 representing 48 distinct tissue and cell types at developmental stages spanning early embryonic (5  
131 days) to mature adult (70 weeks post-hatching). In addition, we accessed a recently published  
132 transcriptional analysis of chick development generated by Cap Analysis of Gene Expression (CAGE)

133 [53], a technique which can be used to quantify gene expression based on the transcript start site [54].  
134 We show that the ‘guilt by association’ approach to functional annotation is viable even when  
135 combining disparate RNA-seq datasets, and utilise the meta-dataset to identify macrophage-specific  
136 and other informative co-expression clusters, providing a resource for genetic and genomic study of  
137 avian trait variation.

138

## 139 **RESULTS**

### 140 ***Selecting samples for inclusion in an RNA-seq meta-dataset***

141 Many chicken RNA-seq datasets are available in public repositories, as detailed in [41]. Robust co-  
142 expression clustering of any two genes depends upon sampling tissues and cells in which both vary  
143 across the widest possible range. To maximise the co-expression signal, we chose datasets to represent  
144 the greatest possible diversity of tissues and organ systems. Not all studies contain links to a publicly  
145 archived dataset, such as a study of induced ochratoxicosis in the kidney cortex [55] and two studies of  
146 the bursa of Fabricius [56, 57]. Samples containing less than 10 million reads were not used, such as  
147 those from a study of the follicular transcriptome throughout the ovulation cycle [58].

148 Datasets used are detailed in Table S1, and have few commonalities: they were sequenced using a  
149 variety of Illumina instruments (HiSeq 2000/2500/3000/4000, Genome Analyzer II/IIx, NextSeq 500  
150 and HiScanSQ), and include single- and paired-end, strand-specific and non-specific, polyA-selected  
151 (mRNA-seq) and rRNA-depleted (total RNA-seq) libraries at different read lengths and depths. For 12  
152 tissues, independently sequenced RNA-seq datasets for the same tissue (Table S2) also allow for  
153 internal tests of the validity of aggregating the data. Throughout this text studies are referred to by  
154 their NCBI BioProject ID.

155

### 156 ***Quantifying expression by iteratively revising a reference transcriptome***

157 Expression was quantified – as transcripts per million (TPM) – using an RNA-seq processing pipeline  
158 [59] which iteratively runs the quantification tool Kallisto [60] with each iteration using an  
159 incrementally revised transcriptome. Kallisto requires that the user provide a set of transcripts, which  
160 are decomposed into k-mers. The expression of each transcript is quantified by matching this set of k-  
161 mers to the k-mers of the reads. For the first iteration of Kallisto, a non-redundant transcriptome  
162 (57,234 transcripts, representing 17,680 Ensembl protein-coding genes) was obtained by combining  
163 Ensembl transcript models with NCBI mRNA RefSeqs (see Materials and Methods).  
164 The output was first parsed for library quality. The reverse cumulative distribution of TPM per gene  
165 was plotted on a log-log scale (Figure 1). The distributions generally approximate a power-law with an  
166 exponent of approximately -1 (Table S3), consistent with Zipf's law (that the probability of an  
167 observation is inversely proportional to its rank) [61, 62]. Four samples with exponents  $< -0.8$  or  $> -$   
168 1.2, i.e. deviating  $> 20\%$  from the optimal value of -1 – were excluded from further analysis (i.e. the  
169 next iteration of Kallisto) (Table S3). Using only data from the useable samples, we created a revised  
170 reference transcriptome. During the first iteration of Kallisto, 55,027 of 57,234 transcripts (96%) were  
171 detectably expressed (average TPM  $> 1$  in at least one tissue, where the average is the median TPM  
172 across all replicates, per BioProject, of that tissue), representing 17,313 Ensembl protein-coding genes  
173 (Table S4). After excluding 2207 transcripts with TPM  $< 1$  in all tissues (Table S5) and those  
174 detectable only in the 4 excluded samples ( $n = 57$ ), a revised transcriptome was generated containing  
175 54,970 transcripts. For the second iteration of Kallisto, expression was re-quantified using this revised  
176 transcriptome, creating a final set of gene-level TPM estimates. The overall meta-dataset provides  
177 gene-level expression for 23,864 gene models (both Ensembl and NCBI) as median TPM across all  
178 replicates, per BioProject, per tissue (Table S6). Of these gene models, 43% (10,090) were  
179 unannotated, having only either an Ensembl placeholder ID or an NCBI locus ID.  
180  
181 ***Randomly down-sampling RNA-seq datasets does not quantitatively alter their expression profiles***

182 Higher resolution expression profiles are dependent upon higher sequencing depths [63] with  
183 diminishing returns – after approximately 10 million reads – on the power to detect genes  
184 differentially expressed between conditions [64]. For the purpose of functional annotation, it is more  
185 important to minimise variation between samples than to comprehensively capture transcripts.  
186 Accordingly, all datasets were randomly down-sampled to exactly 10 million reads before  
187 quantification.  
188 To ensure the resulting co-expression signals are reproducible, it is necessary to establish that there are  
189 no significant differences in expression profiles introduced by sampling. For instance, the LPS-  
190 stimulated BMDM datasets were sequenced at depths of 37.5 to 52.6 million reads, such that when  
191 down-sampling, the BMDM expression profile as quantified for the meta-dataset was obtained using  
192 approximately one fifth to one quarter of the original reads (Table S7). To validate the approach, we  
193 randomly down-sampled each BMDM dataset to 10 million reads 100 times, using seqtk  
194 (<https://github.com/lh3/seqtk>, downloaded 29<sup>th</sup> November 2016) seeded with a random integer  
195 between 0 and 10,000 (Dataset S1). After performing an all-against-all correlation of the 100 sets of  
196 data, the average Spearman’s *rho* was > 0.96 (Table S8), with the absolute difference, per gene,  
197 between maximum and minimum expression level averaging approximately 8 TPM (Figure 2 and  
198 Table S9). 70-75% of the genes detectably expressed (TPM > 1) in at least one of the 100 random  
199 samples were detected in all 100 samples (Table S8). Conversely, <5% of the genes were detectable in  
200 <5% of the samples (Table S8). The detection of these genes was stochastic, as they were expressed at  
201 very low levels – on average, 1.3 TPM (Table S8).

202  
203 ***Biologically meaningful expression profiles are identified even after combining disparate RNA-seq***  
204 ***datasets***  
205 If a meta-analytic approach to RNA-seq is valid, subsets of transcripts enriched in a given tissue  
206 should have annotations functionally appropriate to that tissue. To test this, we calculated a

207 preferential expression measure (PEM) for each gene [65], essentially the median expression divided  
208 by the mean. We then obtained the set of Gene Ontology (GO) terms enriched in each subset of genes  
209 with the highest PEM associated with a particular tissue (Table S10) (see Materials and Methods).  
210 Consistent with the function of each tissue, the bursa of Fabricius (the site of B cell synthesis [66])  
211 showed tissue-specificity for the expression of genes enriched for ‘defence response to bacterium’ ( $p =$   
212  $8.3 \times 10^{-5}$ ), breast muscle for ‘striated muscle contraction’ ( $p = 1.9 \times 10^{-6}$ ), cerebrum for ‘synaptic  
213 transmission’ ( $p = 1.5 \times 10^{-4}$ ), claw epithelium for ‘bone mineralisation’ ( $p = 6.4 \times 10^{-4}$ ), heart for both  
214 ‘muscle contraction’ ( $p = 8.8 \times 10^{-6}$ ) and ‘cellular respiration’ ( $p = 4.6 \times 10^{-15}$ ), kidney for ‘oxidation-  
215 reduction process’ ( $p = 5.3 \times 10^{-5}$ ), pancreas for ‘proteolysis’ ( $p = 0.001$ ), pituitary gland for ‘endocrine  
216 system development’ ( $p = 2 \times 10^{-4}$ ), retina for ‘visual perception’ ( $p = 7.2 \times 10^{-17}$ ), spleen for ‘immune  
217 response’ ( $p = 2.2 \times 10^{-6}$ ), and trachea for ‘cilium morphogenesis’ ( $p < 1 \times 10^{-30}$ ) (Table S10).  
218 In an all-against-all correlation matrix (Pearson’s  $r$ ) (Table S11), the expression profiles of like tissues  
219 were correlated regardless of their BioProject of origin (Table S12). A sample-to-sample network  
220 graph also demonstrates that samples of the same or related tissues cluster together (Figure 3). Taken  
221 together, these results validate the aggregation of data from multiple sources to create an informative  
222 expression atlas.

223

#### 224 ***Signals of co-expression allow for informative functional annotation***

225 Network analysis of the meta-dataset was performed using Miru, a commercial version of BioLayout  
226 *Express<sup>3D</sup>* [67, 68], previously applied to pig [26], sheep [27] and mouse [28] microarray datasets and  
227 CAGE data from the FANTOM5 consortium [24, 25]. A Pearson’s correlation matrix for each gene-  
228 to-gene comparison was visualised as a network graph of 18,127 nodes (genes) linked by 632,038  
229 edges (correlations above a certain threshold; in this case,  $r = 0.8$ ). Clusters of interconnected nodes  
230 represent sets of genes that share a signal of co-expression. These clusters were identified by applying

231 the Markov clustering (MCL) algorithm [69] to the network graph, at an inflation value (which  
232 determines cluster granularity) of 2.2. The contents of each cluster are given in Table S13.

233 Many of the co-expression clusters comprised genes with a tissue- or process-specific expression  
234 profile. Table S14 summarises the highest PEM value for a tissue in each of the clusters with >25  
235 members. Cluster 2 was largely brain-specific: of the 655 genes in this cluster, 281 (43%) had their  
236 highest PEM in the hypothalamus, 155 (24%) had their highest PEM in the cerebrum and 115 (18%)  
237 had their highest PEM in the cerebellum. Other clusters contained genes with expression enriched in  
238 liver (cluster 6), ovary (cluster 7), trachea (cluster 8), testis (cluster 10), retina (clusters 13 and 24),  
239 feather epithelium (cluster 14), breast muscle (cluster 16), kidney (cluster 17), pituitary gland (clusters  
240 19 and 25), *Campylobacter*-infected caecal tonsils (cluster 20), spleen (clusters 21 and 22) and adipose  
241 (cluster 23).

242 The tissues in some of these clusters were represented by multiple independent projects combined in  
243 this meta-atlas. For instance, cluster 6 comprises genes that were enriched in the liver, with data from  
244 three separate BioProjects. Some variation in expression estimates between these independent liver  
245 samples did not affect their inclusion in the same co-expression cluster. Furthermore, the GO terms  
246 enriched in each cluster are functionally consistent with its observed tissue-specificity (Table S15).

247 Some clusters were associated with processes shared by multiple tissues. The largest cluster, cluster 1,  
248 was enriched in embryo-derived samples, and the GO terms are associated strongly with the cell  
249 division cycle and DNA repair (Table S15). The genes within this list include the key transcriptional  
250 regulator, *FOXM1*, and multiple cyclins (*CCNA2/B2B3/C/E1/F* and *J*), and overlap substantially with  
251 cell cycle-associated lists derived from previous cluster analysis [2, 70].

252 We used the ‘guilt by association’ principle to contextualise individual gene annotations – obtained by  
253 protein-level alignment and of varying quality (see Materials and Methods) – as there is an *a priori*  
254 expectation that by virtue of being co-expressed, the genes within a given cluster have related (that is,

255 tissue- or process-specific) functions. In this respect, we can increase confidence in otherwise lower-  
256 quality alignments. Some examples and proposed annotations are summarised in Table S13.  
257 The co-expression profile is especially informative for clusters with few known genes. For instance,  
258 cluster 14 contains 210 genes expressed largely in the feather epithelium (Table S13). 93% of the  
259 genes within this cluster are unannotated, with only 14 genes having a known function (Table 1).  
260 Collectively, the functions of these genes are biologically consistent with an epithelium-enriched  
261 expression profile. Of the 196 unannotated genes, 86% can be aligned to feather keratins (representing  
262 86 of the 96 genes with only an Ensembl ID and 83 of the 100 genes with only an NCBI RefSeq ID)  
263 (Table S13). Other unannotated genes include paralogues of existing genes in the cluster  
264 (ENSGALG00000004358 shares homology with *AMZ1*, ENSGALG00000029002 with *XG* and  
265 LOC428538 with *SDR16C5*), probable members of the keratin-associated protein family, which have  
266 essential roles in hair shaft formation [71] (ENSGALG00000018878, ENSGALG00000044257,  
267 LOC101751162, LOC101751279, LOC107055127, LOC107055128 and LOC107055130), a gene  
268 with homology to the tight junction protein claudin 4 (ENSGALG00000035131) [72], and several  
269 transcripts with homology to uricases (LOC101747367, LOC107056676 and LOC107056678),  
270 enzymes which degrade uric acid (the end point of purine metabolism) [73], notable because purines  
271 act as pigments in avian feathers [74].

272

273 ***Annotation of co-expression clusters associated with innate and acquired immunity and***  
274 ***macrophage biology***

275 The most prominent set of genes co-expressed in macrophages was cluster 4 (n = 458 genes; 129  
276 [28%] are unannotated), in which > 60% of the genes have their highest PEM for BMDMs 24 hours  
277 post-LPS stimulation (Figure 4 and Table S14). This cluster is internally validated by the presence of  
278 transcripts encoding numerous known myeloid effectors/receptors (e.g. *C3AR1*, *CCR2*, *CD40*, *CYBB*,  
279 *CLEC5A*, *DCSTAMP*, *NLRC5*, *METRK*, *MYD88*, *TLR4*), lysosomal components (e.g. *CTSB*, *LAMP1*,

280 *M6PR*) and multiple transcription factors (*BATF3*, *CEBPB*, *IRF1*, *NFE2L2*, *NRR1H3* [also known as  
281 *LXRA*], *SPI1* [also known as *PU.1*], *STAT1*, *TFEC*) that are also macrophage-enriched in mouse and  
282 human [75]. Their co-expression strongly indicates that basic macrophage transcriptional regulation is  
283 conserved between birds and mammals. Accordingly, the provisional annotations of genes that lack an  
284 informative name in this cluster, shown in Table S13, are given extra weight by their association.  
285 Other macrophage clusters include cluster 34 (n = 93 genes; 72 [77%] are unannotated) and cluster 37  
286 (n = 79 genes; 16 [20%] are unannotated), in both of which the majority of genes had their highest  
287 PEM for the HD11 immortalised macrophage cell line (from BioProject PRJEB1406): 98% and 90%,  
288 respectively (Table S14). The smallest macrophage-specific cluster was cluster 84 (n = 26 genes; 19  
289 [73%] are unannotated), in which every gene had its highest PEM for BMDMs treated with CSF1  
290 (from BioProject PRJEB7662) (Table S14).  
291 The *CSF1R* gene was contained within cluster 27 (n = 129 genes, of which 32 [25%] are unannotated),  
292 which had an expression profile shared by both dendritic cells and macrophages. 36% of the genes in  
293 cluster 27 had their highest PEM for dendritic cells and 26% for untreated BMDMs (both samples  
294 from BioProject PRJEB7475), with the remaining 26% for BMDMs treated with CSF1 (from  
295 BioProject PRJEB7662) (Table S14). This cluster also contained the lipopolysaccharide receptor and  
296 commonly used monocyte marker, *CD14*, several genes (*C1QA/B/C*, *MARCO*, *P2RY12/13*, and  
297 *STAB1*) that are associated with tissue-specific macrophage populations in mice [76], and a single  
298 myeloid-associated transcription factor, *MAFB*, which is required for tissue macrophage development  
299 in mice [77]. The cells referred to as dendritic cells are bone marrow cells grown in *GM-CSF* (*CSF2*),  
300 rather than *CSF1*. As noted in previous analyses of mouse [78] and human [79] transcriptomes, cells  
301 differentiated in *GM-CSF* have much more in common with macrophages than with classical dendritic  
302 cells dependent upon *FLT3*-ligand.  
303 The clusters associated with the acquired immune response, predominantly B and T cells, are  
304 somewhat smaller and poorly-annotated (clusters 20, 21, 22, 29 and 78). Cluster 21, expressed most

305 highly in spleen, contains *TIMD4* (ENSGALG00000003876), which promotes T-cell expansion and  
306 survival [80], and is enriched with B cell-associated genes, including the B cell transcription factors  
307 *BATF*, *IRF4*, *PAX5*, *RUNX3*, and *SPIC*, as well as the class II trans-activator *CIITA*, class II subunit  
308 *CD74* and the class II MHC gene *BLB2*. The thymus-enriched cluster 29 contains *CD4*, the  
309 recombination activating genes *RAG1* and *RAG2*, and the T cell transcription factors *LEF1*, *RORC* and  
310 *TCF7*.

311

312 ***Integrating gene expression and protein-protein interaction networks***

313 Biological systems can be functionally organised into many different (and intersecting)  
314 networks based on the nature of their interaction, including – aside from gene co-expression  
315 networks – metabolic/biochemical networks, signal transduction networks, regulatory  
316 networks, and protein-protein interaction (PPI) networks [81]. Data from different networks  
317 can be integrated: for instance, subunits of the same protein complex are known to be co-  
318 expressed [82], with those genes present in both a co-expression and PPI network having a  
319 high probability of performing similar functions [83]. We therefore determined the set of  
320 genes present in both the same co-expression cluster and a PPI network (Table S16),  
321 obtaining chicken PPI data by mapping human PPIs to orthologous chicken genes (see  
322 Materials and Methods). The PPI and co-expression data are mutually supportive. For  
323 example, there were 32 PPIs among the genes in the macrophage-specific cluster 4. These  
324 include *STAT1* (signal transducer and activator of transcription 1-alpha/beta) – a critical  
325 mediator of the pro-inflammatory response of macrophages to LPS [84] – and the  
326 transcription factors *ATF3*, a known inducer of *STAT1* [85], and *SPI1/PU.1*, which is  
327 essential for macrophage differentiation [86]. Also in the network are the tyrosine kinase  
328 *LYN*, which is activated alongside *STAT1* in response to *IL5* (a key mediator of eosinophil  
329 activation [87]), and the adaptor protein *GRB2*, which facilitates the activation of *ERK* by

330 tyrosine kinases [88] (*ERK* signalling is essential to macrophage development [89]). In  
331 addition, the network contained *SOCS3*, a negative regulator of cytokine signalling that  
332 inhibits the nuclear translocation of *STAT1* in response to *IFN* stimulation [90], with this  
333 stimulation a key constituent of classical macrophage activation [91].

334

335 ***Integrating gene expression and promoter expression networks***

336 Relatively few RNA-seq datasets were available for chicken embryonic development. Lizio  
337 *et al.* [53] have recently analysed the time course of chicken development using Cap Analysis  
338 of Gene Expression (CAGE). Their dataset complements a CAGE-based analysis of gene  
339 expression in multiple tissues of the mouse during embryonic development [92]. Network  
340 analysis of the mouse dataset revealed a signature of the expansion of the tissue macrophage  
341 populations during embryonic development, and the inverse relationship between cell  
342 proliferation and tissue-specific differentiation in each organ [93]. Analysis of a macrophage-  
343 specific transgene in birds revealed that, as in mammals, macrophages are first produced by  
344 the yolk sac, progressively infiltrate the embryo and expand in number to become a major  
345 cell population in every organ [33, 94]. The expression atlas we have developed provides a  
346 complementary resource for adult tissues and includes a time course of embryonic  
347 development. By combining the atlas with the CAGE data, it would be possible to infer the  
348 developmental time course of organ systems in the chicken. We obtained the chicken CAGE  
349 data of Lizio *et al.* [53] and clustered the promoter-based expression levels in the same  
350 manner as for the RNA-seq atlas. Figure 5 shows the resulting network graph, and the  
351 average expression profiles of a subset of clusters. Table S17 provides a full list of promoters  
352 in each of the co-expression clusters and their average expression profiles. As discussed by  
353 Lizio, *et al.*, the embryonic CAGE data identify transcription start sites for many tissue-  
354 specific and regulated genes, including developmental regulators such as *brachyury*. The

355 intersection of the CAGE and RNA-seq clusters is presented in Table S18. Not surprisingly,  
356 the largest promoter cluster overlapped substantially with cluster 1 in the RNA-seq atlas  
357 which was embryo-enriched in expression. It contained numerous developmental regulators,  
358 anabolic/cell cycle, and mitochondria-associated genes with an average profile of down-  
359 regulation during development (Figure 5). Aside from the whole embryo profiles, the CAGE  
360 data contains several additional samples, including bone marrow-derived mesenchymal stem  
361 cells (MSC), aortic smooth muscle cells (ASMC), hepatocytes, extra-embryonic tissues and  
362 both leg and wing buds. Each of the samples was enriched for specific promoters that also  
363 varied during development and accordingly defined clusters. Clusters 2 and 10 of the CAGE  
364 data were enriched in MSC and ASMC, and contained many mesenchyme-associated genes  
365 including multiple collagens and other connective tissue-associated transcripts. CAGE  
366 clusters 4 and 9 were hepatocyte-enriched and most likely track the development of the liver  
367 during development. Cluster 4, shown in Figure 5, contains the transcription factor *HNF1A*,  
368 and many of the transcripts within it encode secreted proteins such as complement  
369 components and clotting factors. CAGE cluster 5 (Figure 5) contains the muscle-specific  
370 transcription factors *MYOD1*, *MYOG* and *SOX2*, and numerous skeletal muscle-associated  
371 genes in common with cluster 16 from the RNA-seq atlas, and increases in expression  
372 throughout development. The transcripts within cluster 5 are not expressed in the aortic  
373 smooth muscle cells. CAGE clusters 7, 16, 18 and 19 contained transcripts that were  
374 expressed transiently at different stages of embryonic development, including multiple  
375 members of the *HOX* and *CDX* families. CAGE clusters 8 and 25 both contained promoters  
376 of multiple genes that are expressed specifically in macrophages in the RNA-seq atlas  
377 (clusters 4 and 27). The average expression profiles are shown in Figure 5, with  
378 representative genes indicated. The macrophage-specific transcription factor *SPI1*, and most  
379 other macrophage-enriched genes within CAGE clusters 8 and 25, fall within the larger

380 macrophage-associated clusters (4, 27 and 31) within the RNA-seq atlas. Interestingly,  
381 CAGE cluster 25 appears to be enriched for genes expressed specifically in brain  
382 macrophages (microglia), including *CSF1R*, *C1QA*, *C1QB*, *C1QC*, *CTSS*, *DOCK2*, *HAVCR1*  
383 *LAPTM5*, *LY86*, *MPEG1*, and *P2RY13* [95], which in mice appear to develop from yolk sac  
384 progenitors rather than definitive haematopoiesis [96]. Several other microglia/macrophage-  
385 associated transcripts, notably *CX3CR1*, *P2RY12*, *TIMD4*, and *TREM2*, are detectable in the  
386 CAGE data at the same embryonic stage, but did not cluster because their expression differs  
387 in the cell populations. In each of the macrophage-associated clusters, there were numerous  
388 promoters currently with uninformative annotation, which by inference are likely to be  
389 macrophage-related. Consistent with the location of *CSF1R* mRNA and the *CSF1R*-reporter  
390 gene in the chicken [33], *CSF1R* and *SPI1* were both first detectable in the embryo at  
391 between HH12 and HH14 (day 2), and both increased in parallel during embryonic  
392 development. Figure 6 shows the ZENBU (<http://fantom.gsc.riken.jp/zenbu/>) view of the  
393 chicken *CSF1R* locus, identifying the transcription start site downstream of the *PDGFRB*  
394 locus, and the time course of appearance of *CSF1R* transcripts in the embryo and their  
395 expression in isolated cells. The reason that CAGE clusters 8 and 25 genes separate in the  
396 dataset is that they were also detected at high levels in “mesenchymal stem cells” and to a  
397 varying extent in “hepatocytes” (Figure 5). In mice, macrophages were shown to be a major  
398 contaminant of bone marrow-derived osteoblast cell cultures [97]. Based upon this cluster  
399 analysis in the embryo (which reveals separate mesenchyme and hepatocyte-specific  
400 clusters), and the atlas data, where these genes were clearly macrophage-enriched, the  
401 expression of macrophage-associated genes is almost certainly a reflection of the presence of  
402 large numbers of macrophages in these cell populations. Indeed, the set of promoters active in  
403 “mesenchymal stem cells” was found to be enriched for binding sites for *SPI1* and *CEBPA*,

404 transcription factors that can induce the transdifferentiation of lymphoid precursors into  
405 macrophages [98].

406

407 **DISCUSSION**

408 RNA-seq is a multi-step process of reverse transcription, amplification, fragmentation, purification,  
409 adaptor ligation and sequencing, with each step subject to error [99]. Such laboratory-specific  
410 variation is also independent of intrinsic sequencing biases, which can influence the nucleotide  
411 composition of the reads [100] (leading to mismatches between the sequenced read and the original  
412 RNA fragment [101]), the GC content of the reads [102], and the sequencing error rate [11].

413 Despite all of these constraints, Figure 3 shows that in a sample-to-sample network graph of many  
414 independently sequenced tissues, the signal of co-expression clearly outweighs the noise.

415 The critical step in reducing the noise, and making the datasets comparable, was to down-size the  
416 RNA-seq libraries so that the depth of coverage of the transcriptome was the same in each case.

417 This has the effect of removing a great deal of the stochastic detection of more lowly-expressed  
418 transcripts. Figure 2 and Table S9 show that the random sampling used to down-size does not  
419 substantially alter the relative expression estimates of any two genes within any given sample, with  
420 equivalent expression profiles reconstructed for each of 100 random samples. Combined with the  
421 use of Kallisto to quantify expression, which maps a common depth of k-mers to a standardised  
422 reference transcriptome, the method we have developed effectively ensured that each RNA-seq  
423 library was exploring an equivalent transcriptomic space.

424 The success of the aggregation of public domain data in terms of genome annotation is evident  
425 from the analysis of the membership of co-expression clusters in Table S13. Each cluster clearly  
426 contains genes of known function, shows evidence of very strong GO enrichment, and as noted in  
427 similar array-based studies [2, 26] commonly contains the transcription factors that regulate the

428 other members of the cluster. On that basis, it would be reasonable to provisionally assign the  
429 same GO terms to genes of unknown function, at least within the larger clusters. For example, the  
430 genes within cluster 1 that are not currently functionally annotated or assigned a clear orthologue  
431 are likely to be involved in some way in the cell cycle. Indeed, the provisional annotations of many  
432 of them shown in Table S13 indicate this is very likely to be the case. Similarly, the genes we have  
433 identified that were enriched in innate and acquired immune cells are likely to be associated with  
434 heritable variation in disease resistance/susceptibility.

435 Detailed examination of individual clusters can provide significant biological insights. Cluster 8,  
436 enriched in trachea, and with the second highest expression in lung, was strongly enriched with  
437 GO terms associated with cilium, microtubule binding, motor activity and the actin cytoskeleton  
438 (Table S15), and includes, for example, multiple members of the cilia and flagella-associated  
439 protein (*CFAP*), dynein regulatory complex (*DRC*) and other dynein-related gene families.  
440 Mutations in many of these genes have been associated with human ciliopathies [103]. This cluster  
441 also contained the transcription factor *FOXJ1*, which is essential for the formation of motile cilia  
442 in mice [104]. Provisional annotations of genes of unknown function in this cluster are consistent  
443 with the overall enrichment for genes associated with motility. The presence of the epithelial  
444 transcription factors *ELF5* and *PAX9* in this cluster suggests both could have a role in regulation of  
445 this key gene set, providing a possible reason for the embryonic lethality of the knockouts of each  
446 gene [105, 106]. Interestingly, *KIAA0586*, which is also known as *TALPID3*, is in a separate  
447 smaller cluster – number 139 – that is more widely expressed. The *TALPID3* protein encodes a  
448 centromeric component, and mutation affects the formation of primary, non-motile cilia and  
449 signaling by the morphogen sonic hedgehog [107, 108]. Many of the genes that are apparently co-  
450 regulated with *TALPID3* have been associated in some way with regulatory functions of primary  
451 cilia, including *CEP120* which, like *KIAA0596*, is mutated in human Joubert syndrome [109].  
452 Other members of the cluster may be candidate interactors with *TALPID3*.

453 The validity of the approach, and of the clusters generated, was established by comparing tissue-  
454 and function-specific clusters obtained by an alternate method of quantifying RNA expression  
455 levels, CAGE, using a public dataset of chicken embryo development. This showed that tissue-  
456 specific developmental gene expression can be detected using whole embryos (as we have  
457 previously shown for mouse [93]), and that the genes in the developmental stage clusters matched  
458 those found in the adult tissue atlas.

459 The clustering we have presented is based upon an arbitrary correlation threshold. For every gene  
460 of interest, it can be informative to identify its transcriptional companions. To this end, as we have  
461 done previously for human [2], pig [26], sheep [27] and mouse [28], we have made the current  
462 version of this atlas available as a searchable database using the gene annotation portal BioGPS  
463 [110] (<http://www.biogps.org/chickenatlas>), where one can utilise a simple “find correlated”  
464 function to identify genes with similar expression profiles. In turn, this resource allows a rapid  
465 comparative assessment of the expression of a gene of interest in mammals and birds and the  
466 extent to which functional information is likely to be transferable across species.

467 The advantage of the aggregation method we have applied is that it is can be extended with new  
468 data from tissues and cell types we have not currently included. The larger the dataset, and the  
469 greater the transcriptional space sampled, the more stringent the correlations that will be generated  
470 and the more likely they are to produce new biological insights.

471

472 **MATERIALS AND METHODS**

473 ***Animals***

474 To obtain bone marrow-derived macrophages, nine chickens of approximately 8 weeks of age (3  
475 female and 3 male Ross 308 broilers, and 3 female CSF1R-MacApple transgenic NOVOgen Brown  
476 layers) were euthanized by cervical dislocation and confirmed dead by decapitation. Likewise were  
477 euthanized 23 broiler chickens, each 5 weeks of age, to obtain the caecal tonsils. All animal work was

478 conducted in accordance with guidelines of the Roslin Institute and the University of Edinburgh and  
479 carried out under the regulations of the Animals (Scientific Procedures) Act 1986. Approval was  
480 obtained from the Roslin Institute's and the University of Edinburgh's Protocols and Ethics  
481 Committees.

482

483 ***Macrophage cell culture and RNA isolation***

484 Bone marrow-derived macrophage (BMDM) culture and challenge *in vivo* were performed as  
485 previously described [111]. Chicken bone marrow was cultured for 7 days with 350 ng/μl chicken  
486 CSF1 on Sterilin plastic to differentiate BMDMs. Adherent cells were then transferred to tissue culture  
487 plastic and cells plated at 80% confluence. BMDMs were challenged with the addition of LPS at 100  
488 ng/ml to culture medium and then harvested after 0 (null condition), and 24 hours. Cells were  
489 harvested in TRIzol® (15596018; Thermo Fisher Scientific) and extraction performed with the RNeasy  
490 Mini Kit (74106; Qiagen Hilden, Germany) according to manufacturer's instructions.

491

492 ***Collection of *Campylobacter*-infected caecal tonsils***

493 Birds were naturally exposed to *Campylobacter* spp. under commercial farm conditions. Caeca and  
494 caecal tonsil samples were collected in RNAlater (AM7021; Thermo Fisher Scientific, Waltham,  
495 USA). *Campylobacter* load in caeca was determined by selective culture as previously described  
496 [112]. Seven serial ten-fold dilutions of caecal content were prepared in phosphate-buffered saline and  
497 100 μl plated to mCCDA (modified cefoperazone-deoxycholate agar) supplemented with cefoperazone  
498 (32 mg/L) and amphotericin B (10 mg/L; Oxoid), followed by incubation for 48 hours under  
499 microaerophilic conditions (5% O<sub>2</sub>, 5% CO<sub>2</sub>, and 90% N<sub>2</sub>) at 41C. Dilutions were plated in duplicate  
500 and colonies with morphology typical of *Campylobacter* detected in all samples. RNA was extracted  
501 from the caecal tonsils using the RNeasy Mini Kit (74106; Qiagen Hilden, Germany) according to  
502 manufacturer's instructions. As chickens were exposed naturally rather than being explicitly

503 challenged with *Campylobacter*, bacterial load varied considerably between individuals. Accordingly,  
504 tonsil samples were partitioned into two broad subsets: those from chickens whose caecum has high  
505 *Campylobacter* load ( $\geq 10,000$  CFU/g), and those with low *Campylobacter* load ( $< 10,000$  CFU/g).

506

507 ***RNA-sequencing***

508 For both BMDM and caecal tonsil samples, library preparation was performed by Edinburgh  
509 Genomics. Total RNA (for BMDMs) and mRNA (for caecal tonsils) was, in both cases, sequenced by  
510 Edinburgh Genomics at a depth of  $>40$  million strand-specific 75bp paired-end reads per sample, using  
511 an Illumina HiSeq 4000. The raw data is deposited in the European Nucleotide Archive under  
512 accessions PRJEB22373 (BMDMs) and PRJEB22580 (caecal tonsils).

513

514 ***Public RNA-seq datasets***

515 Publicly accessible datasets used in this study are described in Table S1. The meta-atlas aggregating  
516 these data details, per tissue, the associated NCBI BioProject and Sequence Read Archive (SRA)  
517 sample IDs (Table S6). All public datasets for this study are available via the SRA, a public repository  
518 for sequence data maintained by the International Nucleotide Sequence Database Collaboration  
519 (INSDC) and accessible from the websites of its constituent members: known as the SRA if via the  
520 National Center for Biotechnology Information (NCBI) ([www.ncbi.nlm.nih.gov/sra](http://www.ncbi.nlm.nih.gov/sra)), the DRA (DDBJ  
521 Read Archive) if via the DNA Data Bank of Japan (DDBJ) (<http://trace.ddbj.nig.ac.jp/dra/>), and the  
522 European Nucleotide Archive (ENA) if via the European Bioinformatics Institute (EBI)  
523 ([www.ebi.ac.uk/ena](http://www.ebi.ac.uk/ena)) [113]. For retrieving the raw files used in this study or for expanding this work  
524 with new datasets from novel tissues, note that data are directly accessible in fastq format from the  
525 ENA and DDBJ but only in a binary .sra format from the NCBI. Decompiling the latter into fastq files  
526 – using the fastq-dump tool within the SRA Toolkit  
527 (<https://trace.ncbi.nlm.nih.gov/Traces/sra/sra.cgi?cmd=show&f=software&m=software&s=software>) –

528 is far slower than analysing fastq files with Kallisto, and so forms a bottleneck in the expression atlas  
529 creation pipeline. For this reason, obtaining fastq files in bulk from NCBI is not recommended unless  
530 necessary.

531

532 ***Defining a reference transcriptome and quantifying expression***

533 Prior to expression level quantification, all RNA-seq datasets were randomly down-sampled to 10  
534 million reads using seqtk (<https://github.com/lh3/seqtk>, downloaded 29th November 2016) with  
535 parameter -s 100 (to seed the random number generator). Expression level was then estimated, as  
536 transcripts per million (TPM), using the high-speed quantification tool Kallisto v0.43.1 [60] and  
537 default parameters. For datasets comprising single-end reads, we used parameters -l 100 -s 10;  
538 estimates of the average fragment length and standard deviation of the fragment length, respectively.  
539 Kallisto quantifies expression at the transcript level by building an index of k-mers from a set of  
540 reference transcripts and then mapping the RNA-seq reads to it, matching k-mers generated from the  
541 reads with the k-mers present in the index. Transcript-level TPM estimates are then summarised to the  
542 gene level. A critical aspect of this method is in selecting an appropriate set of reference transcripts for  
543 which expression is quantified. An appropriate value of  $k$  for the index is also required because if  $k$  is  
544 too large relative to read length, there is a higher chance the k-mers of the reads will contain errors (as  
545 read quality decreases towards the 3' end of reads [4]). If the reads generate erroneous k-mers, they  
546 will not match the k-mers of the index. We used a value of  $k = 21$ , which lies – approximately –  
547 between half the length of the shortest read and a third the length of the longest read.

548 As a reference transcriptome, we obtained from Ensembl v89 the set of GalGal5 protein-coding  
549 transcripts, parsing the batch release ([ftp://ftp.ensembl.org/pub/release-89/fasta/gallus\\_gallus/cds/Gallus\\_gallus.Gallus\\_gallus-5.0.cds.all.fa.gz](ftp://ftp.ensembl.org/pub/release-89/fasta/gallus_gallus/cds/Gallus_gallus.Gallus_gallus-5.0.cds.all.fa.gz), accessed 21<sup>st</sup> June 2017) to  
550 retain only those transcripts with the ‘protein-coding’ biotype (n=28,768 transcripts, representing  
551 10,846 genes). To this was added the CDS of 28,466 NCBI mRNA RefSeqs that had neither been

553 assigned Ensembl transcript IDs, nor whose sequence was already present in the Ensembl release  
554 (under any other identifier). To reduce the likelihood of spurious read mapping, CDS < 300 bp were  
555 excluded from analysis. Erroneous expression level estimates are more likely when fewer possible  
556 reads can be derived from a gene, i.e. if the CDS is short [59]. While this approach arguably improves  
557 accuracy, it unavoidably excludes certain families, for instance the gallinacins [114], antimicrobial  
558 peptides known for their short chain lengths [115].

559 Although the Ensembl and NCBI sets of transcripts overlap, there are many unique entries in each. For  
560 example, RefSeqs XM\_015294055 and XM\_015294059 are both predicted transcripts of the  
561 macrophage-marker gene *CD163* [116], although Ensembl refers to this gene only by the numerical ID  
562 ‘418303’. RefSeq records beginning ‘XM’ are produced by the NCBI genome annotation pipeline and  
563 can lack transcript or protein homology support; by contrast, ‘NM’ records are validated [117].  
564 Consequently, neither of the *CD163* RefSeqs are assigned Ensembl transcript IDs, and so they are  
565 excluded from the Ensembl batch release.

566 The RefSeq mRNA set also includes predictions of novel transcript sequences for existing Ensembl  
567 genes. For instance, the chicken *BF1* gene (classical MHC class 1; Ensembl gene ID  
568 ENSGALG00000033932) has 7 transcripts (Ensembl v89), encoding proteins of length 228, 323, 345,  
569 346, 350, 354 and 360 amino acids (aa). However, *BF1* has only 3 associated mRNA RefSeqs, 1  
570 validated and 2 predicted: NM\_001044683, XM\_015294995, and XM\_015294996. These RefSeqs do  
571 not necessarily encode different proteins to those present in Ensembl – rather, the RefSeq mRNAs  
572 incorporate untranslated regions (UTRs) and so can encapsulate Ensembl CDS. For instance, the  
573 validated RefSeq mRNA NM\_001044683 encodes the same 360aa protein as Ensembl CDS  
574 ENSGALT00000066783 (i.e. the same transcript model is independently available from both  
575 resources), but the RefSeq nucleotide sequence extends 17 bases upstream (the 5’ UTR) and 146 bases  
576 downstream (the 3’ UTR) of the coding ORF. By contrast, XM\_015294995 encodes a putative 356aa  
577 peptide (XP\_015150481) and XM\_015294996 a 349aa peptide (XP\_015150482), neither of which are

578 available from Ensembl. As the XM\_015294996 mRNA – an automated prediction – fully  
579 incorporates ENSGALT00000086848 (the CDS encoding the 228aa *BF1* protein), we considered the  
580 sequence better supported by the Ensembl model, as Ensembl takes a conservative approach to  
581 annotation [118], and the predicted peptide spurious. By contrast, the XM\_015294995 mRNA does  
582 not contain any existing Ensembl CDS and so encodes a protein absent from Ensembl.  
583 Overall, we retained RefSeq ‘XM’ mRNAs only if they can be assigned to a gene not yet present in  
584 the Ensembl annotation, or, if that gene is present, they do not incorporate a CDS from any of that  
585 gene’s Ensembl transcript models. UTRs were trimmed from each RefSeq mRNA by excluding all  
586 sequence outside the longest ORF. This combined set of Ensembl and RefSeq transcripts constitutes a  
587 standardised RNA space against which expression can be quantified, as in [59].  
588 After quantifying expression with this initial transcriptome, a revised transcriptome was created,  
589 excluding those transcripts whose average TPM was < 1 in all tissues (Table S5), or which were only  
590 detectable in one tissue (as these may be artefacts of differential sequencing depth). Tissues whose  
591 distribution of TPM estimates does not comply with Zipf’s law (see below) were not counted. The  
592 revised transcriptome contains 28,276 Ensembl transcripts (representing 10,826 Ensembl genes) and  
593 26,694 NCBI transcripts (which account for only 4665 existing Ensembl genes).

594

#### 595 ***Compliance of RNA-seq datasets with Zipf’s law***

596 In a correctly prepared RNA-seq dataset, a minority of reads will produce the majority of reads and so  
597 its distribution of gene-level TPM estimates should comply, to a reasonable approximation, with  
598 Zipf’s law (which states that the probability of an observation is inversely proportional to its rank). A  
599 custom Perl script was used to identify, per sample, the number of unique TPM values and the number  
600 of genes with a TPM at or exceeding this level. After excluding, for robustness, data from the first and  
601 last order of magnitude (as in [119]) and all values of TPM < 5 (which have a higher likelihood of  
602 transcriptional noise), the data was log-transformed and a linear regression model fitted using R v3.2.0

603 [120]. Samples whose exponents deviated too greatly from -1 (by  $\pm 20\%$ , i.e. if the exponent is  $< -0.8$   
604 or  $> -1.2$ ) were considered erroneous.

605

606 ***Tissue specificity***

607 For each gene, we calculated a preferential expression measure (PEM) in a manner similar to [65].  
608 PEM relates the average expression of that gene in a given tissue to the average expression of that  
609 gene in all tissues. For each gene  $i$ , then for tissue  $t_i$ ,  $\text{PEM}(t_i) = S - A$ , where  $S$  = expression of gene  $i$  in  
610 tissue  $t_i$ , and  $A$  = arithmetic mean expression of gene  $i$  across the set of all tissues. Prior to calculation,  
611 all TPM values  $< 1$  were considered to be 1, and a  $\log_2$ -transformation applied. This is to ensure that  
612 genes with expression indistinguishable from noise (TPM  $< 1$ ) will have a PEM of 0. Each gene will  
613 have a distribution of PEM values, one for each tissue in the meta-datasets. Genes with higher PEM  
614 values for a given tissue are more tissue-specific in their expression profile.

615

616 ***Gene Ontology (GO) term enrichment***

617 GO term enrichment was assessed using the R package topGO [121], which utilises the ‘weight’  
618 algorithm to account for the nested structure of the GO tree [122]. topGO requires a reference set of  
619 GO terms, which was built manually from the GalGal5 set (obtained from Ensembl BioMart v89  
620 [123]) and filtered to remove those terms with evidence codes NAS (non-traceable author statement)  
621 or ND (no biological data available), and those assigned to fewer than 10 genes in total. Significantly  
622 enriched GO terms ( $p < 0.05$ ) are reported only if the observed number per tissue exceeds the expected  
623 by 2-fold or greater.

624

625 ***Gene annotation***

626 Unannotated genes in GalGal5 – those with only an Ensembl placeholder ID, rather than an HGNC  
627 name – are annotated by reference to the NCBI non-redundant (nr) peptide database v77 [124], with

628 each annotation assigned a quality category of 1 to 8 (highest to lowest quality, respectively), as  
629 previously described [27]. For each unannotated gene, we took the longest encoded peptide and  
630 obtained the set of blastp alignments [125] against NCBI nr, at a scoring threshold of  $p \leq 1e^{-25}$ . These  
631 alignments are a set of possible gene descriptions, of which only one can be selected as the annotation  
632 of that gene. The lowest quality category, 8, is the blastp hit with the lowest E-value. All subsequent  
633 quality categories require higher-quality hits, which: (a) have a % identity within the aligned region of  
634  $\geq 90\%$ , (b) have an alignment length  $\geq 90\%$  of the length of the query protein, (c) have an  
635 alignment length  $\geq 50$  amino acids, (d) have no gaps, and (e) are not to a protein labelled either 'low  
636 quality', 'hypothetical', 'unnamed', 'uncharacterized' or 'putative', or otherwise having a third-party  
637 annotation (as these can be by inference and not experiment). Quality category 7 is the best-scoring  
638 (i.e. lowest E-value) of these higher quality hits. Category 6 is as above, but with at least one  
639 identifiable hit to the human proteome. Category 5 requires that the set of alignments span at least 4  
640 different genera (excluding *Gallus*). At this point, if  $\geq 75\%$  of the alignments have the same  
641 description, the gene is named for the associated HGNC name (according to  
642 [ftp://ftp.ebi.ac.uk/pub/databases/genenames/new/tsv/locus\\_types/gene\\_with\\_protein\\_product.txt](ftp://ftp.ebi.ac.uk/pub/databases/genenames/new/tsv/locus_types/gene_with_protein_product.txt),  
643 downloaded 24<sup>th</sup> August 2016). However, as NCBI nr aggregates multiple sources of data, gene  
644 descriptions have numerous synonyms and so it is not always possible to automatically assign an  
645 HGNC symbol. The highest quality categories, 1 to 4, not only meet the above criteria but have  
646 degrees of reciprocal % identity to the human proteome. The highest quality category, 1, is if there is  
647 also a near-perfect match to an existing, related, peptide (alignment length  $\geq 90\%$  of the length of a  
648 human protein). Other quality categories, in descending order, are: 2 (alignment length  $\geq 75\%$  of the  
649 length of a human protein), 3 ( $\geq 50\%$ ), and 4 ( $< 50\%$ ). Human protein sequences were obtained from  
650 genebuild GRCh38.p8  
651 ([ftp://ftp.ncbi.nlm.nih.gov/genomes/all/GCF\\_000001405.34\\_GRCh38.p8/GCF\\_000001405.34\\_GRCh](ftp://ftp.ncbi.nlm.nih.gov/genomes/all/GCF_000001405.34_GRCh38.p8/GCF_000001405.34_GRCh)  
652 38.p8\_protein.faa.gz, downloaded 30<sup>th</sup> August 2016).

653

654 ***Network analysis***

655 Network analysis was performed using Miru (Kajeka Ltd, Edinburgh, UK), a commercial version of  
656 BioLayout Express<sup>3D</sup> [67, 68]. Miru determines the similarities between individual expression profiles  
657 by building a correlation matrix for both gene-to-gene and sample-to-sample comparisons. This matrix  
658 is then filtered to remove all correlations below a certain threshold (for the gene-to-gene comparison in  
659 the RNA-seq atlas, Pearson's  $r < 0.8$ ). A network graph is constructed by connecting nodes (genes)  
660 with edges (correlations above the threshold), and its local structure interpreted by applying the  
661 Markov clustering (MCL) algorithm [69] at an inflation value (which determines cluster granularity)  
662 of 2.2.

663

664 ***Protein-protein interactions***

665 Protein-protein interaction data was obtained from the IID (Integrated Interactions Database)  
666 version 2017-04 (<http://iid.ophid.utoronto.ca/iid>, accessed 25th July 2017) [126], a resource  
667 which combines computationally predicted PPIs with experimentally determined PPIs drawn  
668 from multiple databases. These include BIND (Biomolecular Interaction Network Database)  
669 [127], BioGRID (Biological General Repository for Interaction Datasets) [128], DIP  
670 (Database of Interacting Proteins) [129], HPRD (Human Protein Reference Database) [130],  
671 IntAct [131], I2D (Interologous Interaction Database) [132], InnateDB [133] and MINT  
672 (Molecular Interaction Database) [134]. The format of the PPI data is as a list of UniProt IDs,  
673 with one of three evidence types for the interaction: 'exp' (experimentally determined in this  
674 species), 'pred' (an *in silico* prediction from one of four previous studies [135-138]) and  
675 'ortho' (predicted by mapping experimentally determined PPIs from another species to  
676 orthologous protein pairs in this species). As chicken PPI data is unavailable, we obtained  
677 human PPIs from the IID, and considered only those PPIs that (a) involve genes that each

678 have a one-to-one orthologue to the chicken with an orthology confidence score of 1 (using  
679 data from Ensembl Compara [139], a score of 1 indicates compliance with the gene tree), a  
680 reciprocal % gene identity of  $\geq 75\%$ , a whole genome alignment score of  $\geq 75\%$ , and a  
681 gene order conservation score of  $\geq 75\%$  (indicating a high degree of contiguity around the  
682 gene of interest), (b) have UniProt IDs that are unambiguously assigned to only one human  
683 gene ID (and thereby only one orthologous chicken gene ID), and (c) have PPI evidence type  
684 ‘exp’ or ‘pred’.

685

#### 686 *Availability of datasets*

687 To test whether down-sampling quantitatively alters the expression profile of an RNA-seq dataset, we  
688 randomly down-sampled each of the 18 BMDM datasets (+/- LPS) to 10 million reads 100 times,  
689 using seqtk seeded with a random integer between 0 and 10,000. These sets of expression estimates  
690 are available as Dataset S1, hosted on the University of Edinburgh DataShare portal  
691 (<http://dx.doi.org/10.7488/ds/2137>). The meta-atlas of chicken gene expression is available in full as  
692 Table S6 and via the cross-species annotation portal BioGPS  
693 ([http://biogps.org/dataset/BDS\\_00031/chicken-atlas/](http://biogps.org/dataset/BDS_00031/chicken-atlas/)). To compare genes between species and to  
694 visualise expression profiles, BioGPS requires that each gene have an Entrez ID, although this is not  
695 the case for all genes in GalGal5. The expression profiles of those genes without Entrez IDs can be  
696 found in Table S6.

697

#### 698 *Analysis of chicken developmental samples*

699 The expression data derived from CAGE [53] were obtained from  
700 [http://fantom.gsc.riken.jp/5/suppl/Lizio\\_et\\_al\\_2017/data](http://fantom.gsc.riken.jp/5/suppl/Lizio_et_al_2017/data); the expression file is named  
701 galGal5.cage\_peak\_tpm.osc.txt.gz and the annotation file galGal5.cage\_peak\_ann.txt. The annotation  
702 and expression files were emerged based on chromosomal location of the promoter. All promoters

703 where no sample exceeded 10 tags per million (tagsPM) were excluded from the analysis. The  
704 expression data were then entered into Miru (as described above), using a correlation coefficient  
705 threshold of 0.75. 22,839 nodes joined by 5,035,102 edges were entered into the analysis and clustered  
706 with an MCL inflation value of 2.2, resulting in 132 clusters of at least 10 nodes.

707

## 708 **DECLARATIONS**

### 709 ***Funding***

710 This work was supported by a Biotechnology and Biological Sciences Research Council (BBSRC)  
711 project grant (BB/M011925/1) to DAH and institute strategic program grants 'Farm Animal  
712 Genomics' (BBS/E/D/20211550) and 'Transcriptomes, Networks and Systems' (BBS/E/D/20211552).  
713 RNA-seq of the *Campylobacter*-infected chickens was supported by funding from the Rural and  
714 Environmental Science and Analytical Sciences Division of the Scottish Government, and from a  
715 BBSRC LINK project with Aviagen Ltd. (BB/J006815/1). Edinburgh Genomics is partly supported  
716 through core grants from the BBSRC (BB/J004243/1), Natural Environmental Research Council  
717 (R8/H10/56), and Medical Research Council (MR/K001744/1). The funders had no role in study  
718 design, data collection and analysis, decision to publish, or preparation of the manuscript.

719

### 720 ***Availability of data and materials***

721 The datasets generated during this study are available in the European Nucleotide Archive under  
722 accessions PRJEB22373 and PRJEB22580. All data analysed during this study are included in this  
723 published article (and its supplementary information files). The atlas of chicken gene expression is  
724 also available via the cross-species annotation portal BioGPS  
725 ([http://biogps.org/dataset/BDS\\_00031/chicken-atlas/](http://biogps.org/dataset/BDS_00031/chicken-atlas/)).

726

### 727 ***Authors' contributions***

728 DAH coordinated the study. LF, AJM, and JOD performed macrophage cell culture and RNA  
729 extraction. AP, JS and MS, funded, generated and provided RNA-seq data from the caecal tonsils of  
730 *Campylobacter*-infected birds. CW and CA prepared data for visualisation with BioGPS. SJB  
731 performed all bioinformatic analyses with the exception of the CAGE analysis. KMS performed the  
732 CAGE analysis. SJB and DAH wrote the manuscript. All authors read, contributed to, and approved  
733 the final manuscript.

734

735 ***Competing interests***

736 The authors declare they have no competing interests.

737

738 ***Consent for publication***

739 Not applicable.

740

741 ***Ethics approval and consent to participate***

742 Approval was obtained from The Roslin Institute's and the University of Edinburgh's Protocols and  
743 Ethics Committees. All animal work was carried out under the regulations of the Animals (Scientific  
744 Procedures) Act 1986.

745

746 **REFERENCES**

747

- 748 1. He F, Yoo S, Wang D, Kumari S, Gerstein M, Ware D, Maslov S: **Large-scale atlas**  
749 **of microarray data reveals the distinct expression landscape of different tissues**  
750 **in *Arabidopsis*.** *Plant J* 2016, **86**(6):472-480.
- 751 2. Mabbott NA, Baillie JK, Brown H, Freeman TC, Hume DA: **An expression atlas of**  
752 **human primary cells: inference of gene function from coexpression networks.**  
753 *BMC Genomics* 2013, **14**(1):1-13.
- 754 3. Doig TN, Hume DA, Theocharidis T, Goodlad JR, Gregory CD, Freeman TC:  
755 **Coexpression analysis of large cancer datasets provides insight into the cellular**  
756 **phenotypes of the tumour microenvironment.** *BMC Genomics* 2013, **14**:469.

757 4. Conesa A, Madrigal P, Tarazona S, Gomez-Cabrero D, Cervera A, McPherson A,  
758 Szcześniak MW, Gaffney DJ, Elo LL, Zhang X *et al*: **A survey of best practices for**  
759 **RNA-seq data analysis.** *Genome Biology* 2016, **17**:13.

760 5. van Dijk EL, Jaszczyszyn Y, Thermes C: **Library preparation methods for next-**  
761 **generation sequencing: Tone down the bias.** *Experimental Cell Research* 2014,  
762 **322**(1):12-20.

763 6. Chhangawala S, Rudy G, Mason CE, Rosenfeld JA: **The impact of read length on**  
764 **quantification of differentially expressed genes and splice junction detection.**  
765 *Genome Biology* 2015, **16**(1):131.

766 7. Sinha R, Lenser T, Jahn N, Gausmann U, Friedel S, Szafranski K, Huse K, Rosenstiel  
767 P, Hampe J, Schuster S *et al*: **TassDB2 - A comprehensive database of subtle**  
768 **alternative splicing events.** *BMC Bioinformatics* 2010, **11**(1):1-7.

769 8. Zhao S, Zhang Y, Gordon W, Quan J, Xi H, Du S, von Schack D, Zhang B:  
770 **Comparison of stranded and non-stranded RNA-seq transcriptome profiling and**  
771 **investigation of gene overlap.** *BMC Genomics* 2015, **16**(1):675.

772 9. Sultan M, Amstislavskiy V, Risch T, Schuette M, Dökel S, Ralser M, Balzereit D,  
773 Lehrach H, Yaspo M-L: **Influence of RNA extraction methods and library**  
774 **selection schemes on RNA-seq data.** *BMC Genomics* 2014, **15**(1):1-13.

775 10. Quail MA, Smith M, Coupland P, Otto TD, Harris SR, Connor TR, Bertoni A,  
776 Swerdlow HP, Gu Y: **A tale of three next generation sequencing platforms:**  
777 **comparison of Ion Torrent, Pacific Biosciences and Illumina MiSeq sequencers.**  
778 *BMC Genomics* 2012, **13**(1):341.

779 11. Li S, Tighe SW, Nicolet CM, Grove D, Levy S, Farmerie W, Viale A, Wright C,  
780 Schweitzer PA, Gao Y *et al*: **Multi-platform assessment of transcriptome profiling**  
781 **using RNA-seq in the ABRF next-generation sequencing study.** *Nat Biotech* 2014,  
782 **32**(9):915-925.

783 12. González E, Joly S: **Impact of RNA-seq attributes on false positive rates in**  
784 **differential expression analysis of de novo assembled transcriptomes.** *BMC*  
785 *Research Notes* 2013, **6**(1):503.

786 13. Adiconis X, Borges-Rivera D, Satija R, DeLuca DS, Busby MA, Berlin AM,  
787 Sivachenko A, Thompson DA, Wysoker A, Fennell T *et al*: **Comparative analysis of**  
788 **RNA sequencing methods for degraded or low-input samples.** *Nat Methods* 2013,  
789 **10**(7):623-629.

790 14. Esteve-Codina A, Arpi O, Martínez-García M, Pineda E, Mallo M, Gut M, Carrato C,  
791 Rovira A, Lopez R, Tortosa A *et al*: **A Comparison of RNA-Seq Results from**  
792 **Paired Formalin-Fixed Paraffin-Embedded and Fresh-Frozen Glioblastoma**  
793 **Tissue Samples.** *PLoS one* 2017, **12**(1):e0170632.

794 15. Gallego Romero I, Pai AA, Tung J, Gilad Y: **RNA-seq: impact of RNA degradation**  
795 **on transcript quantification.** *BMC Biology* 2014, **12**(1):42.

796 16. Seear PJ, Sweeney GE: **Stability of RNA isolated from post-mortem tissues of**  
797 **Atlantic salmon (Salmo salar L.).** *Fish Physiol Biochem* 2008, **34**(1):19-24.

798 17. Opitz L, Salinas-Riester G, Grade M, Jung K, Jo P, Emons G, Ghadimi BM,  
799 Beißbarth T, Gaedcke J: **Impact of RNA degradation on gene expression profiling.**  
800 *BMC Medical Genomics* 2010, **3**(1):36.

801 18. Johnson BR, Atallah J, Plachetzki DC: **The importance of tissue specificity for**  
802 **RNA-seq: highlighting the errors of composite structure extractions.** *BMC*  
803 *Genomics* 2013, **14**(1):586.

804 19. Brawand D, Soumillon M, Necsulea A, Julien P, Csardi G, Harrigan P, Weier M,  
805 Liechti A, Aximu-Petri A, Kircher M *et al*: **The evolution of gene expression levels**  
806 **in mammalian organs.** *Nature* 2011, **478**(7369):343-348.

807 20. Lin S, Lin Y, Nery JR, Urich MA, Breschi A, Davis CA, Dobin A, Zaleski C, Beer  
808 MA, Chapman WC *et al*: **Comparison of the transcriptional landscapes between**  
809 **human and mouse tissues**. *Proceedings of the National Academy of Sciences of the*  
810 *United States of America* 2014, **111**(48):17224-17229.

811 21. Merkin J, Russell C, Chen P, Burge CB: **Evolutionary dynamics of gene and**  
812 **isoform regulation in Mammalian tissues**. *Science (New York, NY)* 2012,  
813 **338**(6114):1593-1599.

814 22. Sudmant PH, Alexis MS, Burge CB: **Meta-analysis of RNA-seq expression data**  
815 **across species, tissues and studies**. *Genome Biology* 2015, **16**(1):287.

816 23. Oliver S: **Guilt-by-association goes global**. *Nature* 2000, **403**(6770):601-603.

817 24. Andersson R, Gebhard C, Miguel-Escalada I, Hoof I, Bornholdt J, Boyd M, Chen Y,  
818 Zhao X, Schmidl C, Suzuki T *et al*: **An atlas of active enhancers across human cell**  
819 **types and tissues**. *Nature* 2014, **507**(7493):455-461.

820 25. Forrest AR, Kawaji H, Rehli M, Baillie JK, de Hoon MJ, Haberle V, Lassmann T,  
821 Kulakovskiy IV, Lizio M, Itoh M *et al*: **A promoter-level mammalian expression**  
822 **atlas**. *Nature* 2014, **507**(7493):462-470.

823 26. Freeman TC, Ivens A, Baillie JK, Beraldi D, Barnett MW, Dorward D, Downing A,  
824 Fairbairn L, Kapetanovic R, Raza S *et al*: **A gene expression atlas of the domestic**  
825 **pig**. *BMC Biology* 2012, **10**(1):1-22.

826 27. Clark EL, Bush SJ, McCulloch MEB, Farquhar IL, Young R, Lefevre L, Pridans C,  
827 Tsang HG, Wu C, Afrasiabi C *et al*: **A high resolution atlas of gene expression in**  
828 **the domestic sheep (Ovis aries)**. *PLOS Genetics* 2017, **13**(9):e1006997.

829 28. Hume DA, Summers KM, Raza S, Baillie JK, Freeman TC: **Functional clustering**  
830 **and lineage markers: insights into cellular differentiation and gene function**  
831 **from large-scale microarray studies of purified primary cell populations**.  
832 *Genomics* 2010, **95**(6):328-338.

833 29. Carpanini SM, Wishart TM, Gillingwater TH, Manson JC, Summers KM: **Analysis of**  
834 **gene expression in the nervous system identifies key genes and novel candidates**  
835 **for health and disease**. *Neurogenetics* 2017, **18**(2):81-95.

836 30. Eising E, Huisman SM, Mahfouz A, Vijfhuizen LS, Anttila V, Winsvold BS, Kurth T,  
837 Ikram MA, Freilinger T, Kaprio J *et al*: **Gene co-expression analysis identifies brain**  
838 **regions and cell types involved in migraine pathophysiology: a GWAS-based**  
839 **study using the Allen Human Brain Atlas**. *Human genetics* 2016, **135**(4):425-439.

840 31. Stern CD: **The chick; a great model system becomes even greater**. *Dev Cell* 2005,  
841 **8**(1):9-17.

842 32. Intarapat S, Stern CD: **Chick stem cells: current progress and future prospects**.  
843 *Stem Cell Res* 2013, **11**(3):1378-1392.

844 33. Balic A, Garcia-Morales C, Vervelde L, Gilhooley H, Sherman A, Garceau V,  
845 Gutowska MW, Burt DW, Kaiser P, Hume DA *et al*: **Visualisation of chicken**  
846 **macrophages using transgenic reporter genes: insights into the development of**  
847 **the avian macrophage lineage**. *Development* 2014, **141**(16):3255-3265.

848 34. Han JY, Lee HJ: **Genome Editing Mediated by Primordial Germ Cell in Chicken**.  
849 *Methods in molecular biology (Clifton, NJ)* 2017, **1630**:153-163.

850 35. Woodcock ME, Idoko-Akoh A, McGrew MJ: **Gene editing in birds takes flight**.  
851 *Mamm Genome* 2017.

852 36. Taylor L, Carlson DF, Nandi S, Sherman A, Fahrenkrug SC, McGrew MJ: **Efficient**  
853 **TALEN-mediated gene targeting of chicken primordial germ cells**. *Development*  
854 2017, **144**(5):928-934.

855 37. Kranis A, Gheyas AA, Boschiero C, Turner F, Yu L, Smith S, Talbot R, Pirani A,  
856 Brew F, Kaiser P *et al*: **Development of a high density 600K SNP genotyping array**  
857 **for chicken.** *BMC Genomics* 2013, **14**:59.

858 38. Cheng HH, Kaiser P, Lamont SJ: **Integrated genomic approaches to enhance**  
859 **genetic resistance in chickens.** *Annu Rev Anim Biosci* 2013, **1**:239-260.

860 39. Kuo RI, Tseng E, Eory L, Paton IR, Archibald AL, Burt DW: **Normalized long read**  
861 **RNA sequencing in chicken reveals transcriptome complexity similar to human.**  
862 *BMC Genomics* 2017, **18**(1):323.

863 40. Kapetanovic R, Fairbairn L, Beraldi D, Sester DP, Archibald AL, Tuggle CK, Hume  
864 **DA: Pig Bone Marrow-Derived Macrophages Resemble Human Macrophages in**  
865 **Their Response to Bacterial Lipopolysaccharide.** *The Journal of Immunology*  
866 2012, **188**(7):3382-3394.

867 41. Smith J, Burt DW, the Avian RC: **The Avian RNAseq Consortium: a community**  
868 **effort to annotate the chicken genome.** *Cytogenetic and genome research* 2015,  
869 **145**(2):78-179.

870 42. Langouet-Astrie CJ, Meinsen AL, Grunwald ER, Turner SD, Enke RA: **RNA**  
871 **sequencing analysis of the developing chicken retina.** *Scientific Data* 2016,  
872 **3**:160117.

873 43. Piórkowska K, Żukowski K, Nowak J, Połtowicz K, Ropka-Molik K, Gurgul A:  
874 **Genome-wide RNA-Seq analysis of breast muscles of two broiler chicken groups**  
875 **differing in shear force.** *Animal Genetics* 2016, **47**(1):68-80.

876 44. Wu P, Ng CS, Yan J, Lai Y-C, Chen C-K, Lai Y-T, Wu S-M, Chen J-J, Luo W,  
877 Widelitz RB *et al*: **Topographical mapping of  $\alpha$ - and  $\beta$ -keratins on developing**  
878 **chicken skin integuments: Functional interaction and evolutionary perspectives.**  
879 *Proceedings of the National Academy of Sciences* 2015, **112**(49):E6770-E6779.

880 45. Resnyk CW, Chen C, Huang H, Wu CH, Simon J, Le Bihan-Duval E, Duclos MJ,  
881 Cogburn LA: **RNA-Seq Analysis of Abdominal Fat in Genetically Fat and Lean**  
882 **Chickens Highlights a Divergence in Expression of Genes Controlling Adiposity,**  
883 **Hemostasis, and Lipid Metabolism.** *PloS one* 2015, **10**(10):e0139549.

884 46. Shen X, Bai X, Xu J, Zhou M, Xu H, Nie Q, Lu X, Zhang X: **Transcriptome**  
885 **sequencing reveals genetic mechanisms underlying the transition between the**  
886 **laying and brooding phases and gene expression changes associated with**  
887 **divergent reproductive phenotypes in chickens.** *Molecular Biology Reports* 2016,  
888 **43**(9):977-989.

889 47. Pritchett EM, Lamont SJ, Schmidt CJ: **Transcriptomic changes throughout post-**  
890 **hatch development in Gallus gallus pituitary.** *Journal of Molecular Endocrinology*  
891 2016, **58**(1):43-55.

892 48. Van Goor A, Ashwell CM, Persia ME, Rothschild MF, Schmidt CJ, Lamont SJ:  
893 **Unique genetic responses revealed in RNA-seq of the spleen of chickens**  
894 **stimulated with lipopolysaccharide and short-term heat.** *PloS one* 2017,  
895 **12**(2):e0171414.

896 49. Wang Y, Lupiani B, Reddy SM, Lamont SJ, Zhou H: **RNA-seq analysis revealed**  
897 **novel genes and signaling pathway associated with disease resistance to avian**  
898 **influenza virus infection in chickens.** *Poultry Science* 2014, **93**(2):485-493.

899 50. Li Z, Ouyang H, Zheng M, Cai B, Han P, Abdalla BA, Nie Q, Zhang X: **Integrated**  
900 **Analysis of Long Non-coding RNAs (LncRNAs) and mRNA Expression Profiles**  
901 **Reveals the Potential Role of LncRNAs in Skeletal Muscle Development of the**  
902 **Chicken.** *Frontiers in Physiology* 2016, **7**:687.

903 51. Muret K, Klopp C, Wucher V, Esquerré D, Legeai F, Lecerf F, Désert C, Boutin M,  
904 Jehl F, Acloque H *et al*: **Long noncoding RNA repertoire in chicken liver and**  
905 **adipose tissue.** *Genetics, selection, evolution : GSE* 2017, **49**:6.

906 52. Roux P-F, Frésard L, Boutin M, Leroux S, Klopp C, Djari A, Esquerré D, Martin  
907 PGP, Zerjal T, Gourichon D *et al*: **The Extent of mRNA Editing Is Limited in**  
908 **Chicken Liver and Adipose, but Impacted by Tissular Context, Genotype, Age,**  
909 **and Feeding as Exemplified with a Conserved Edited Site in COG3.** *G3:*  
910 *Genes/Genomes/Genetics* 2016, **6**(2):321-335.

911 53. Lizio M, Deviatiiarov R, Nagai H, Galan L, Arner E, Itoh M, Lassmann T, Kasukawa  
912 T, Hasegawa A, Ros MA *et al*: **Systematic analysis of transcription start sites in**  
913 **avian development.** *PLoS biology* 2017, **15**(9):e2002887.

914 54. Deviatiiarov R, Lizio M, Gusev O: **Application of a CAGE Method to an Avian**  
915 **Development Study.** *Methods in molecular biology (Clifton, NJ)* 2017, **1650**:101-  
916 109.

917 55. Zeferino CP, Wells KD, Moura ASAMT, Rottinghaus GE, Ledoux DR: **Changes in**  
918 **renal gene expression associated with induced ochratoxicosis in chickens:**  
919 **activation and deactivation of transcripts after varying durations of exposure.**  
920 *Poultry Science* 2017, **96**(6):1855-1865.

921 56. Han D, Zhang Y, Chen J, Hua G, Li J, Deng X, Deng X: **Transcriptome analyses of**  
922 **differential gene expression in the bursa of Fabricius between Silky Fowl and**  
923 **White Leghorn.** *Scientific Reports* 2017, **7**:45959.

924 57. Liu X-d, Zhang F, Shan H, Wang S-b, Chen P-Y: **mRNA expression in different**  
925 **developmental stages of the chicken bursa of Fabricius.** *Poultry Science* 2016,  
926 **95**(8):1787-1794.

927 58. Zhu G, Mao Y, Zhou W, Jiang Y: **Dynamic Changes in the Follicular**  
928 **Transcriptome and Promoter DNA Methylation Pattern of Steroidogenic Genes**  
929 **in Chicken Follicles throughout the Ovulation Cycle.** *PloS one* 2016,  
930 **10**(12):e0146028.

931 59. Bush SJ, McCulloch MEB, Summers KM, Hume DA, Clark EL: **Integration of**  
932 **quantitated expression estimates from polyA-selected and rRNA-depleted RNA-**  
933 **seq libraries.** *BMC Bioinformatics* 2017, **18**(1):301.

934 60. Bray NL, Pimentel H, Melsted P, Pachter L: **Near-optimal probabilistic RNA-seq**  
935 **quantification.** *Nat Biotech* 2016, **34**(5):525-527.

936 61. Lu T, Costello CM, Croucher PJ, Hasler R, Deuschl G, Schreiber S: **Can Zipf's law**  
937 **be adapted to normalize microarrays?** *BMC Bioinformatics* 2005, **6**:37.

938 62. Furusawa C, Kaneko K: **Zipf's law in gene expression.** *Phys Rev Lett* 2003,  
939 **90**(8):088102.

940 63. Tarazona S, García-Alcalde F, Dopazo J, Ferrer A, Conesa A: **Differential**  
941 **expression in RNA-seq: A matter of depth.** *Genome Research* 2011, **21**(12):2213-  
942 2223.

943 64. Liu Y, Zhou J, White KP: **RNA-seq differential expression studies: more sequence**  
944 **or more replication?** *Bioinformatics* 2014, **30**(3):301-304.

945 65. Huminiecki L, Lloyd A, Wolfe K: **Congruence of tissue expression profiles from**  
946 **Gene Expression Atlas, SAGEmap and TissueInfo databases.** *BMC Genomics*  
947 2003, **4**(1):31.

948 66. Glick B: **Historical perspective: the bursa of Fabricius and its influence on B-cell**  
949 **development, past and present.** *Vet Immunol Immunopathol* 1991, **30**(1):3-12.

950 67. Freeman TC, Goldovsky L, Brosch M, van Dongen S, Maziere P, Grocock RJ,  
951 Freilich S, Thornton J, Enright AJ: **Construction, visualisation, and clustering of**

transcription networks from microarray expression data. *PLoS computational biology* 2007, **3**(10):2032-2042.

68. Theocharidis A, van Dongen S, Enright AJ, Freeman TC: **Network visualization and analysis of gene expression data using BioLayout Express(3D)**. *Nature protocols* 2009, **4**(10):1535-1550.

69. van Dongen S, Abreu-Goodger C: **Using MCL to extract clusters from networks**. *Methods in molecular biology (Clifton, NJ)* 2012, **804**:281-295.

70. Bar-Joseph Z, Siegfried Z, Brandeis M, Brors B, Lu Y, Eils R, Dynlacht BD, Simon I: **Genome-wide transcriptional analysis of the human cell cycle identifies genes differentially regulated in normal and cancer cells**. *Proceedings of the National Academy of Sciences of the United States of America* 2008, **105**(3):955-960.

71. Wu D-D, Irwin DM, Zhang Y-P: **Molecular evolution of the keratin associated protein gene family in mammals, role in the evolution of mammalian hair**. *BMC evolutionary biology* 2008, **8**(1):241.

72. Eckelhoefer HA, Rajapaksa TE, Wang J, Hamer M, Appleby NC, Ling J, Lo DD: **Claudin-4: Functional Studies Beyond the Tight Junction**. In: *Claudins: Methods and Protocols*. Edited by Turksen K. Totowa, NJ: Humana Press; 2011: 115-128.

73. So A, Thorens B: **Uric acid transport and disease**. *The Journal of Clinical Investigation* 2010, **120**(6):1791-1799.

74. Galvan I, Solano F: **Bird Integumentary Melanins: Biosynthesis, Forms, Function and Evolution**. *Int J Mol Sci* 2016, **17**(4):520.

75. Hume DA, Summers KM, Rehli M: **Transcriptional Regulation and Macrophage Differentiation**. *Microbiol Spectr* 2016, **4**(3).

76. Mass E, Ballesteros I, Farlik M, Halbritter F, Gunther P, Crozet L, Jacome-Galarza CE, Handler K, Klughammer J, Kobayashi Y *et al*: **Specification of tissue-resident macrophages during organogenesis**. *Science (New York, NY)* 2016, **353**(6304).

77. Aziz A, Soucie E, Sarrazin S, Sieweke MH: **MafB/c-Maf deficiency enables self-renewal of differentiated functional macrophages**. *Science (New York, NY)* 2009, **326**(5954):867-871.

78. Hume DA, Mabbott N, Raza S, Freeman TC: **Can DCs be distinguished from macrophages by molecular signatures?** *Nature immunology* 2013, **14**(3):187-189.

79. Joshi A, Pooley C, Freeman TC, Lennartsson A, Babina M, Schmidl C, Geijtenbeek T, Michoel T, Severin J, Itoh M *et al*: **Technical Advance: Transcription factor, promoter, and enhancer utilization in human myeloid cells**. *Journal of leukocyte biology* 2015, **97**(5):985-995.

80. Rodriguez-Manzanet R, Meyers JH, Balasubramanian S, Slavik J, Kassam N, Dardalhon V, Greenfield EA, Anderson AC, Sobel RA, Hafler DA *et al*: **TIM-4 Expressed on APCs Induces T Cell Expansion and Survival**. *The Journal of Immunology* 2008, **180**(7):4706.

81. Pavlopoulos GA, Secrier M, Moschopoulos CN, Soldatos TG, Kossida S, Aerts J, Schneider R, Bagos PG: **Using graph theory to analyze biological networks**. *BioData Mining* 2011, **4**:10-10.

82. Jansen R, Greenbaum D, Gerstein M: **Relating whole-genome expression data with protein-protein interactions**. *Genome Res* 2002, **12**(1):37-46.

83. Tornow S, Mewes HW: **Functional modules by relating protein interaction networks and gene expression**. *Nucleic acids research* 2003, **31**(21):6283-6289.

84. Kovarik P, Stoiber D, Novy M, Decker T: **Stat1 combines signals derived from IFN-gamma and LPS receptors during macrophage activation**. *The EMBO Journal* 1998, **17**(13):3660-3668.

1001 85. Kim JY, Song EH, Lee S, Lim JH, Choi JS, Koh IU, Song J, Kim WH: **The**  
1002 **induction of STAT1 gene by activating transcription factor 3 contributes to**  
1003 **pancreatic beta-cell apoptosis and its dysfunction in streptozotocin-treated mice.**  
1004 *Cell Signal* 2010, **22**(11):1669-1680.

1005 86. Celada A, Borras FE, Soler C, Lloberas J, Klemsz M, van Beveren C, McKercher S,  
1006 Maki RA: **The transcription factor PU.1 is involved in macrophage proliferation.**  
1007 *J Exp Med* 1996, **184**(1):61-69.

1008 87. Pazdrak K, Justement L, Alam R: **Mechanism of inhibition of eosinophil activation**  
1009 **by transforming growth factor-beta. Inhibition of Lyn, MAP, Jak2 kinases and**  
1010 **STAT1 nuclear factor.** *J Immunol* 1995, **155**(9):4454-4458.

1011 88. Frühbeck G: **Intracellular signalling pathways activated by leptin.** *Biochemical*  
1012 *Journal* 2006, **393**(Pt 1):7-20.

1013 89. Richardson ET, Shukla S, Nagy N, Boom WH, Beck RC, Zhou L, Landreth GE,  
1014 Harding CV: **ERK Signaling Is Essential for Macrophage Development.** *PLoS one*  
1015 2015, **10**(10):e0140064.

1016 90. Song MM, Shuai K: **The suppressor of cytokine signaling (SOCS) 1 and SOCS3**  
1017 **but not SOCS2 proteins inhibit interferon-mediated antiviral and**  
1018 **antiproliferative activities.** *J Biol Chem* 1998, **273**(52):35056-35062.

1019 91. Su X, Yu Y, Zhong Y, Giannopoulou EG, Hu X, Liu H, Cross JR, Ratsch G, Rice  
1020 CM, Ivashkiv LB: **Interferon-gamma regulates cellular metabolism and mRNA**  
1021 **translation to potentiate macrophage activation.** *Nature immunology* 2015,  
1022 **16**(8):838-849.

1023 92. Arner E, Daub CO, Vitting-Seerup K, Andersson R, Lilje B, Drablos F, Lennartsson  
1024 A, Ronnerblad M, Hrydziszko O, Vitezic M *et al*: **Transcribed enhancers lead**  
1025 **waves of coordinated transcription in transitioning mammalian cells.** *Science*  
1026 (*New York, NY*) 2015, **347**(6225):1010-1014.

1027 93. Summers KM, Hume DA: **Identification of the macrophage-specific promoter**  
1028 **signature in FANTOM5 mouse embryo developmental time course data.** *Journal*  
1029 *of leukocyte biology* 2017.

1030 94. Garceau V, Balic A, Garcia-Morales C, Sauter KA, McGrew MJ, Smith J, Vervelde  
1031 L, Sherman A, Fuller TE, Oliphant T *et al*: **The development and maintenance of**  
1032 **the mononuclear phagocyte system of the chick is controlled by signals from the**  
1033 **macrophage colony-stimulating factor receptor.** *BMC Biol* 2015, **13**:12.

1034 95. Gautier EL, Shay T, Miller J, Greter M, Jakubzick C, Ivanov S, Helft J, Chow A,  
1035 Elpek KG, Gordonov S *et al*: **Gene-expression profiles and transcriptional**  
1036 **regulatory pathways that underlie the identity and diversity of mouse tissue**  
1037 **macrophages.** *Nature immunology* 2012, **13**(11):1118-1128.

1038 96. Epelman S, Lavine KJ, Randolph GJ: **Origin and functions of tissue macrophages.**  
1039 *Immunity* 2014, **41**(1):21-35.

1040 97. Chang MK, Raggatt LJ, Alexander KA, Kuliwaba JS, Fazzalari NL, Schroder K,  
1041 Maylin ER, Ripoll VM, Hume DA, Pettit AR: **Osteal tissue macrophages are**  
1042 **intercalated throughout human and mouse bone lining tissues and regulate**  
1043 **osteoblast function in vitro and in vivo.** *J Immunol* 2008, **181**(2):1232-1244.

1044 98. Feng R, Desbordes SC, Xie H, Tillo ES, Pixley F, Stanley ER, Graf T: **PU.1 and**  
1045 **C/EBP $\alpha$ / $\beta$  convert fibroblasts into macrophage-like cells.** *Proceedings of the*  
1046 *National Academy of Sciences* 2008, **105**(16):6057-6062.

1047 99. Li X, Nair A, Wang S, Wang L: **Quality control of RNA-seq experiments.** *Methods*  
1048 *in molecular biology (Clifton, NJ)* 2015, **1269**:137-146.

1049 100. Hansen KD, Brenner SE, Dudoit S: **Biases in Illumina transcriptome sequencing**  
1050 **caused by random hexamer priming.** *Nucleic acids research* 2010, **38**(12):e131-  
1051 e131.

1052 101. van Gurp TP, McIntyre LM, Verhoeven KJF: **Consistent Errors in First Strand**  
1053 **cDNA Due to Random Hexamer Mispriming.** *PloS one* 2013, **8**(12):e85583.

1054 102. Risso D, Schwartz K, Sherlock G, Dudoit S: **GC-Content Normalization for RNA-**  
1055 **Seq Data.** *BMC Bioinformatics* 2011, **12**(1):480.

1056 103. Reiter JF, Leroux MR: **Genes and molecular pathways underpinning ciliopathies.**  
1057 *Nat Rev Mol Cell Biol* 2017.

1058 104. Stauber M, Boldt K, Wrede C, Weidemann M, Kellner M, Schuster-Gossler K,  
1059 Kuhnel MP, Hegermann J, Ueffing M, Gossler A: **1700012B09Rik, a FOXJ1**  
1060 **effector gene active in ciliated tissues of the mouse but not essential for motile**  
1061 **ciliogenesis.** *Dev Biol* 2017.

1062 105. Zhou J, Chehab R, Tkalcevic J, Naylor MJ, Harris J, Wilson TJ, Tsao S, Tellis I,  
1063 Zavarsek S, Xu D *et al:* **Elf5 is essential for early embryogenesis and mammary**  
1064 **gland development during pregnancy and lactation.** *EMBO J* 2005, **24**(3):635-644.

1065 106. Kist R, Greally E, Peters H: **Derivation of a mouse model for conditional**  
1066 **inactivation of Pax9.** *Genesis* 2007, **45**(7):460-464.

1067 107. Bangs F, Antonio N, Thongnuek P, Welten M, Davey MG, Briscoe J, Tickle C:  
1068 **Generation of mice with functional inactivation of talpid3, a gene first identified**  
1069 **in chicken.** *Development* 2011, **138**(15):3261-3272.

1070 108. Yin Y, Bangs F, Paton IR, Prescott A, James J, Davey MG, Whitley P, Genikhovich  
1071 G, Technau U, Burt DW *et al:* **The Talpid3 gene (KIAA0586) encodes a**  
1072 **centrosomal protein that is essential for primary cilia formation.** *Development*  
1073 2009, **136**(4):655-664.

1074 109. Roosing S, Romani M, Isrie M, Rosti RO, Micalizzi A, Musaev D, Mazza T, Al-  
1075 Gazali L, Altunoglu U, Boltshauser E *et al:* **Mutations in CEP120 cause Joubert**  
1076 **syndrome as well as complex ciliopathy phenotypes.** *J Med Genet* 2016, **53**(9):608-  
1077 615.

1078 110. Wu C, Jin X, Tsueng G, Afrasiabi C, Su AI: **BioGPS: building your own mash-up**  
1079 **of gene annotations and expression profiles.** *Nucleic acids research* 2016,  
1080 **44**(D1):D313-D316.

1081 111. Garcia-Morales C, Nandi S, Zhao D, Sauter KA, Vervelde L, McBride D, Sang HM,  
1082 Clinton M, Hume DA: **Cell-autonomous sex differences in gene expression in**  
1083 **chicken bone marrow-derived macrophages.** *J Immunol* 2015, **194**(5):2338-2344.

1084 112. Psifidi A, Fife M, Howell J, Matika O, van Diemen PM, Kuo R, Smith J, Hocking  
1085 PM, Salmon N, Jones MA *et al:* **The genomic architecture of resistance to**  
1086 **Campylobacter jejuni intestinal colonisation in chickens.** *BMC Genomics* 2016,  
1087 **17**:293.

1088 113. Kodama Y, Shumway M, Leinonen R: **The Sequence Read Archive: explosive**  
1089 **growth of sequencing data.** *Nucleic acids research* 2012, **40**(Database issue):D54-  
1090 56.

1091 114. Lynn DJ, Higgs R, Gaines S, Tierney J, James T, Lloyd AT, Fares MA, Mulcahy G,  
1092 O'Farrelly C: **Bioinformatic discovery and initial characterisation of nine novel**  
1093 **antimicrobial peptide genes in the chicken.** *Immunogenetics* 2004, **56**(3):170-177.

1094 115. Le C-F, Gudimella R, Razali R, Manikam R, Sekaran SD: **Transcriptome analysis of**  
1095 **Streptococcus pneumoniae treated with the designed antimicrobial peptides,**  
1096 **DM3.** *Scientific Reports* 2016, **6**:26828.

1097 116. Fabriek BO, Dijkstra CD, van den Berg TK: **The macrophage scavenger receptor**  
1098 **CD163.** *Immunobiology* 2005, **210**(2):153-160.

1099 117. O'Leary NA, Wright MW, Brister JR, Ciufo S, Haddad D, McVeigh R, Rajput B,  
1100 Robbertse B, Smith-White B, Ako-Adjei D *et al*: **Reference sequence (RefSeq)**  
1101 **database at NCBI: current status, taxonomic expansion, and functional**  
1102 **annotation.** *Nucleic acids research* 2016, **44**(D1):D733-745.

1103 118. Curwen V, Eyras E, Andrews TD, Clarke L, Mongin E, Searle SMJ, Clamp M: **The**  
1104 **Ensembl Automatic Gene Annotation System.** *Genome Research* 2004, **14**(5):942-  
1105 950.

1106 119. Balwierz PJ, Carninci P, Daub CO, Kawai J, Hayashizaki Y, Van Belle W, Beisel C,  
1107 van Nimwegen E: **Methods for analyzing deep sequencing expression data:**  
1108 **constructing the human and mouse promoterome with deepCAGE data.** *Genome*  
1109 *Biol* 2009, **10**(7):R79.

1110 120. **R: A Language and Environment for Statistical Computing** [<http://www.R-project.org>]

1111 121. **topGO: Enrichment analysis for Gene Ontology**  
1112 [<http://www.bioconductor.org/packages/release/bioc/html/topGO.html>]

1113 122. Alexa A, Rahnenführer J, Lengauer T: **Improved scoring of functional groups from**  
1114 **gene expression data by decorrelating GO graph structure.** *Bioinformatics* 2006,  
1115 **22**(13):1600-1607.

1116 123. Kinsella RJ, Kahari A, Haider S, Zamora J, Proctor G, Spudich G, Almeida-King J,  
1117 Staines D, Derwent P, Kerhornou A *et al*: **Ensembl BioMarts: a hub for data**  
1118 **retrieval across taxonomic space.** *Database : the journal of biological databases*  
1119 *and curation* 2011, **2011**:bar030.

1120 124. Pruitt KD, Tatusova T, Maglott DR: **NCBI Reference Sequence (RefSeq): a**  
1121 **curated non-redundant sequence database of genomes, transcripts and proteins.**  
1122 *Nucleic acids research* 2005, **33**(Database Issue):D501-D504.

1123 125. Altschul SF, Madden TL, Schäffer AA, Zhang J, Zhang Z, Miller W, Lipman DJ:  
1124 **Gapped BLAST and PSI-BLAST: a new generation of protein database search**  
1125 **programs.** *Nucleic acids research* 1997, **25**(17):3389-3402.

1126 126. Kotlyar M, Pastrello C, Sheahan N, Jurisica I: **Integrated interactions database:**  
1127 **tissue-specific view of the human and model organism interactomes.** *Nucleic*  
1128 *acids research* 2016, **44**(D1):D536-541.

1129 127. Bader GD, Betel D, Hogue CWV: **BIND: the Biomolecular Interaction Network**  
1130 **Database.** *Nucleic acids research* 2003, **31**(1):248-250.

1131 128. Chatr-Aryamontri A, Breitkreutz BJ, Oughtred R, Boucher L, Heinicke S, Chen D,  
1132 Stark C, Breitkreutz A, Kolas N, O'Donnell L *et al*: **The BioGRID interaction**  
1133 **database: 2015 update.** *Nucleic acids research* 2015, **43**(Database issue):D470-478.

1134 129. Salwinski L, Miller CS, Smith AJ, Pettit FK, Bowie JU, Eisenberg D: **The Database**  
1135 **of Interacting Proteins: 2004 update.** *Nucleic acids research* 2004, **32**(Database  
1136 issue):D449-451.

1137 130. Keshava Prasad TS, Goel R, Kandasamy K, Keerthikumar S, Kumar S, Mathivanan S,  
1138 Telikicherla D, Raju R, Shafreen B, Venugopal A *et al*: **Human Protein Reference**  
1139 **Database--2009 update.** *Nucleic acids research* 2009, **37**(Database issue):D767-772.

1140 131. Hermjakob H, Montecchi-Palazzi L, Lewington C, Mudali S, Kerrien S, Orchard S,  
1141 Vingron M, Roechert B, Roepstorff P, Valencia A *et al*: **IntAct: an open source**  
1142 **molecular interaction database.** *Nucleic acids research* 2004, **32**(Database  
1143 issue):D452-D455.

1144 132. Brown KR, Jurisica I: **Unequal evolutionary conservation of human protein**  
1145 **interactions in interologous networks.** *Genome Biol* 2007, **8**(5):R95.

1147 133. Lynn DJ, Winsor GL, Chan C, Richard N, Laird MR, Barsky A, Gardy JL, Roche  
1148 FM, Chan TH, Shah N *et al*: **InnateDB: facilitating systems-level analyses of the**  
1149 **mammalian innate immune response.** *Mol Syst Biol* 2008, **4**:218.

1150 134. Chatr-aryamontri A, Ceol A, Palazzi LM, Nardelli G, Schneider MV, Castagnoli L,  
1151 Cesareni G: **MINT: the Molecular INTERaction database.** *Nucleic acids research*  
1152 2007, **35**(Database issue):D572-D574.

1153 135. Rhodes DR, Tomlins SA, Varambally S, Mahavisno V, Barrette T, Kalyana-  
1154 Sundaram S, Ghosh D, Pandey A, Chinnaiyan AM: **Probabilistic model of the**  
1155 **human protein-protein interaction network.** *Nature biotechnology* 2005,  
1156 **23**(8):951-959.

1157 136. Elefsinioti A, Sarac OS, Hegele A, Plake C, Hubner NC, Poser I, Sarov M, Hyman A,  
1158 Mann M, Schroeder M *et al*: **Large-scale de novo prediction of physical protein-**  
1159 **protein association.** *Molecular & cellular proteomics : MCP* 2011, **10**(11):M111  
1160 010629.

1161 137. Zhang QC, Petrey D, Deng L, Qiang L, Shi Y, Thu CA, Bisikirska B, Lefebvre C,  
1162 Accili D, Hunter T *et al*: **Structure-based prediction of protein-protein**  
1163 **interactions on a genome-wide scale.** *Nature* 2012, **490**(7421):556-560.

1164 138. Kotlyar M, Pastrello C, Pivetta F, Lo Sardo A, Cumbaa C, Li H, Naranian T, Niu Y,  
1165 Ding Z, Vafaee F *et al*: **In silico prediction of physical protein interactions and**  
1166 **characterization of interactome orphans.** *Nat Methods* 2015, **12**(1):79-84.

1167 139. Vilella AJ, Severin J, Ureta-Vidal A, Heng L, Durbin R, Birney E:  
1168 **EnsemblCompara GeneTrees: Complete, duplication-aware phylogenetic trees**  
1169 **in vertebrates.** *Genome Res* 2009, **19**(2):327-335.

1170 140. Diaz-Perales A, Quesada V, Peinado JR, Ugalde AP, Alvarez J, Suarez MF, Gomis-  
1171 Ruth FX, Lopez-Otin C: **Identification and characterization of human**  
1172 **archaemetzincin-1 and -2, two novel members of a family of metalloproteases**  
1173 **widely distributed in Archaea.** *J Biol Chem* 2005, **280**(34):30367-30375.

1174 141. Jiang TX, Tuan TL, Wu P, Widelitz RB, Chuong CM: **From buds to follicles:**  
1175 **matrix metalloproteinases in developmental tissue remodeling during feather**  
1176 **morphogenesis.** *Differentiation* 2011, **81**(5):307-314.

1177 142. Takeda M, Obara N, Suzuki Y: **Keratin filaments of epithelial and taste-bud cells**  
1178 **in the circumvallate papillae of adult and developing mice.** *Cell and Tissue*  
1179 *Research* 1990, **260**(1):41-48.

1180 143. Plowman GD, Green JM, McDonald VL, Neubauer MG, Disteche CM, Todaro GJ,  
1181 Shoyab M: **The amphiregulin gene encodes a novel epidermal growth factor-**  
1182 **related protein with tumor-inhibitory activity.** *Mol Cell Biol* 1990, **10**(5):1969-  
1183 1981.

1184 144. Günzel D, Yu ASL: **Claudins and the Modulation of Tight Junction Permeability.**  
1185 *Physiological Reviews* 2013, **93**(2):525-569.

1186 145. Quinn LM, Kilpatrick LM, Latham SE, Kalionis B: **Homeobox genes DLX4 and**  
1187 **HB24 are expressed in regions of epithelial-mesenchymal cell interaction in the**  
1188 **adult human endometrium.** *Mol Hum Reprod* 1998, **4**(5):497-501.

1189 146. Alibardi L, Holthaus KB, Sukserree S, Hermann M, Tschachler E, Eckhart L:  
1190 **Immunolocalization of a Histidine-Rich Epidermal Differentiation Protein in the**  
1191 **Chicken Supports the Hypothesis of an Evolutionary Developmental Link**  
1192 **between the Embryonic Subepidermis and Feather Barbs and Barbules.** *PloS one*  
1193 2016, **11**(12):e0167789.

1194 147. Lopes Ricardo J, Johnson James D, Toomey Matthew B, Ferreira Mafalda S, Araujo  
1195 Pedro M, Melo-Ferreira J, Andersson L, Hill Geoffrey E, Corbo Joseph C, Carneiro

1196 M: **Genetic Basis for Red Coloration in Birds.** *Current Biology* 2016, **26**(11):1427-1434.

1198 148. Strasser B, Mlitz V, Hermann M, Rice RH, Eigenheer RA, Alibardi L, Tschachler E, Eckhart L: **Evolutionary Origin and Diversification of Epidermal Barrier Proteins in Amniotes.** *Molecular Biology and Evolution* 2014, **31**(12):3194-3205.

1200 149. Holmes RS: **Vertebrate patatin-like phospholipase domain-containing protein 4 (PNPLA4) genes and proteins: a gene with a role in retinol metabolism.** *3 Biotech* 2012, **2**(4):277-286.

1202 150. Long AC, Bomser JA, Grzybowski DM, Chandler HL: **All-Trans Retinoic Acid Regulates Cx43 Expression, Gap Junction Communication and Differentiation in Primary Lens Epithelial Cells.** *Current Eye Research* 2010, **35**(8):670-679.

1204 151. Wasmeier C, Romao M, Plowright L, Bennett DC, Raposo G, Seabra MC: **Rab38 and Rab32 control post-Golgi trafficking of melanogenic enzymes.** *J Cell Biol* 2006, **175**(2):271-281.

1206 152. Coppola U, Annona G, D'Aniello S, Ristoratore F: **Rab32 and Rab38 genes in chordate pigmentation: an evolutionary perspective.** *BMC evolutionary biology* 2016, **16**(1):26.

1208 153. Wang F, Feng Y, Li P, Wang K, Feng L, Liu Y-F, Huang H, Guo Y-B, Mao Q-S, Xue W-J: **RASSF10 is an epigenetically inactivated tumor suppressor and independent prognostic factor in hepatocellular carcinoma.** *Oncotarget* 2016, **7**(4):4279-4297.

1210 154. Lee S-A, Belyaeva OV, Kedishvili NY: **Biochemical characterization of human epidermal retinol dehydrogenase 2.** *Chemico-Biological Interactions* 2009, **178**(1):182-187.

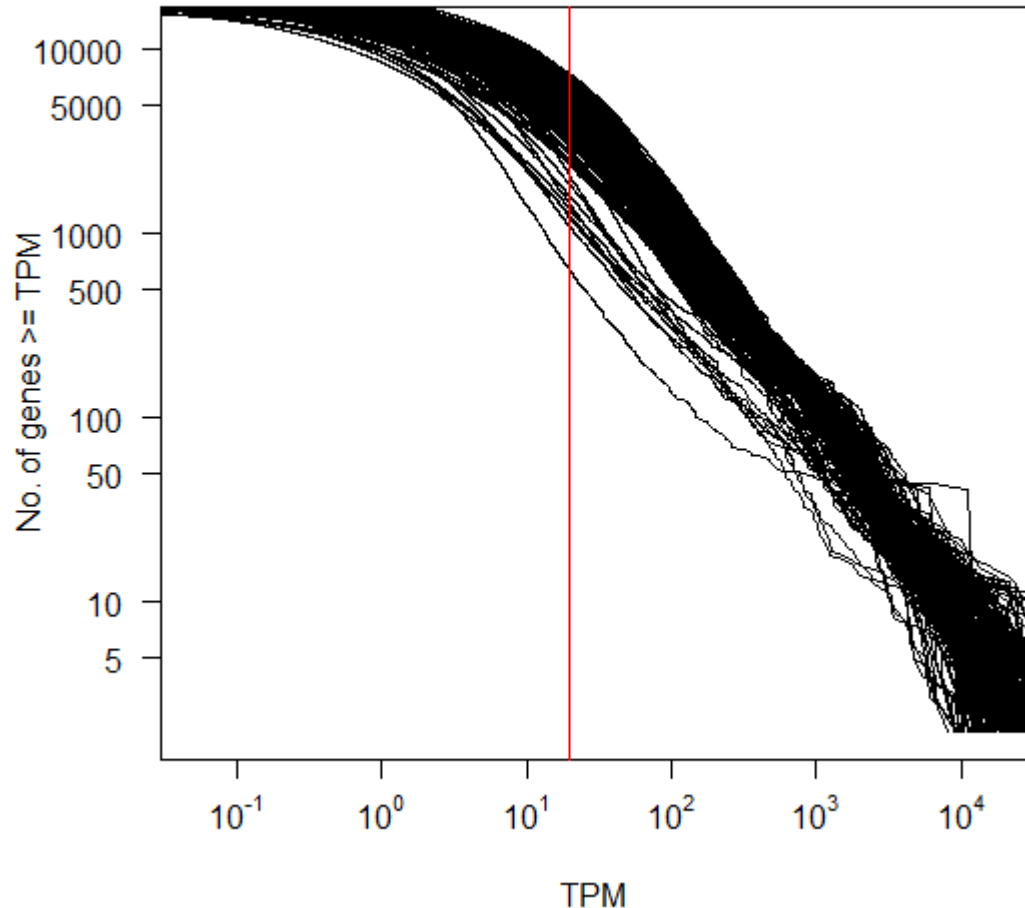
1212 155. Johnson NC: **XG: the forgotten blood group system.** *Immunohematology* 2011, **27**(2):68-71.

1222

1223

1224 **FIGURES**

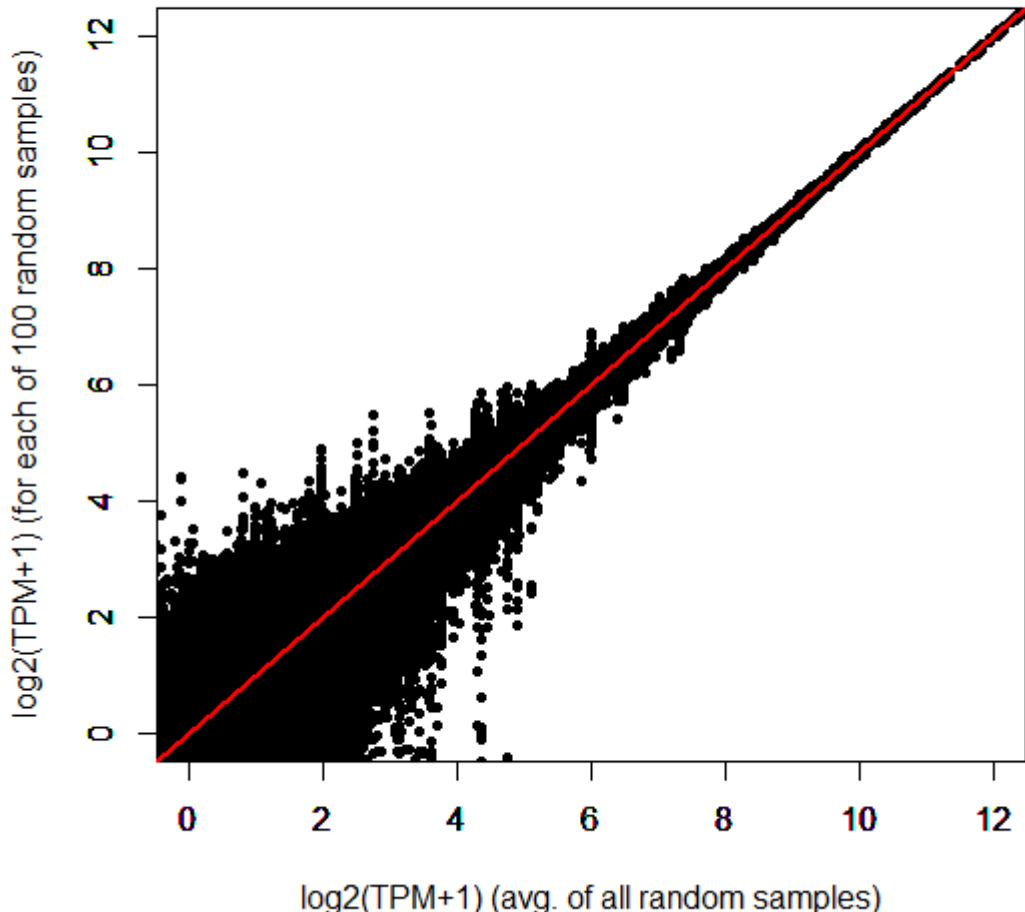
1225



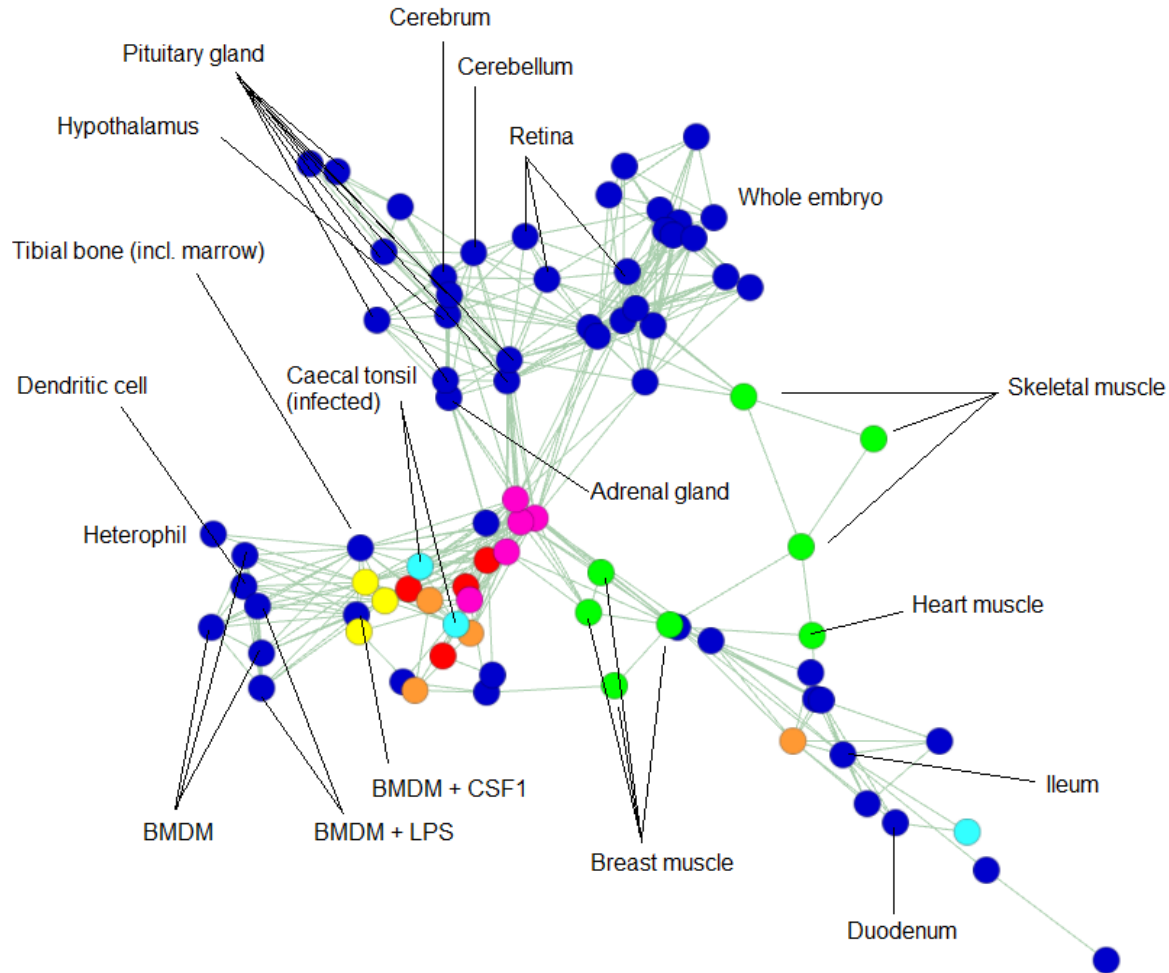
1226

1227 **Figure 1.** Reverse cumulative distribution of the number of genes that have at least a given TPM. Both  
1228 axes are logarithmic. Each line represents data from an individual SRA sample ID, quantified using  
1229 the first iteration Kallisto transcriptome (i.e. a non-redundant set of Ensembl protein-coding CDS plus  
1230 trimmed RefSeq mRNAs). Samples are not otherwise distinguished as in general, most relationships  
1231 approximate the same power-law: a minority of genes account for the majority of reads. These  
1232 relationships are piecewise linear because the capture of lowly expressed genes is noisy, an artefact of  
1233 random transcriptome sampling. The vertical red line denotes TPM = 5. At higher values of TPM, the

1234 majority of samples have a log-linear relationship. Those that do not are erroneous, and are excluded  
1235 from subsequent analysis. Exponents of each sample's log-log plot are given in Table S3.  
1236



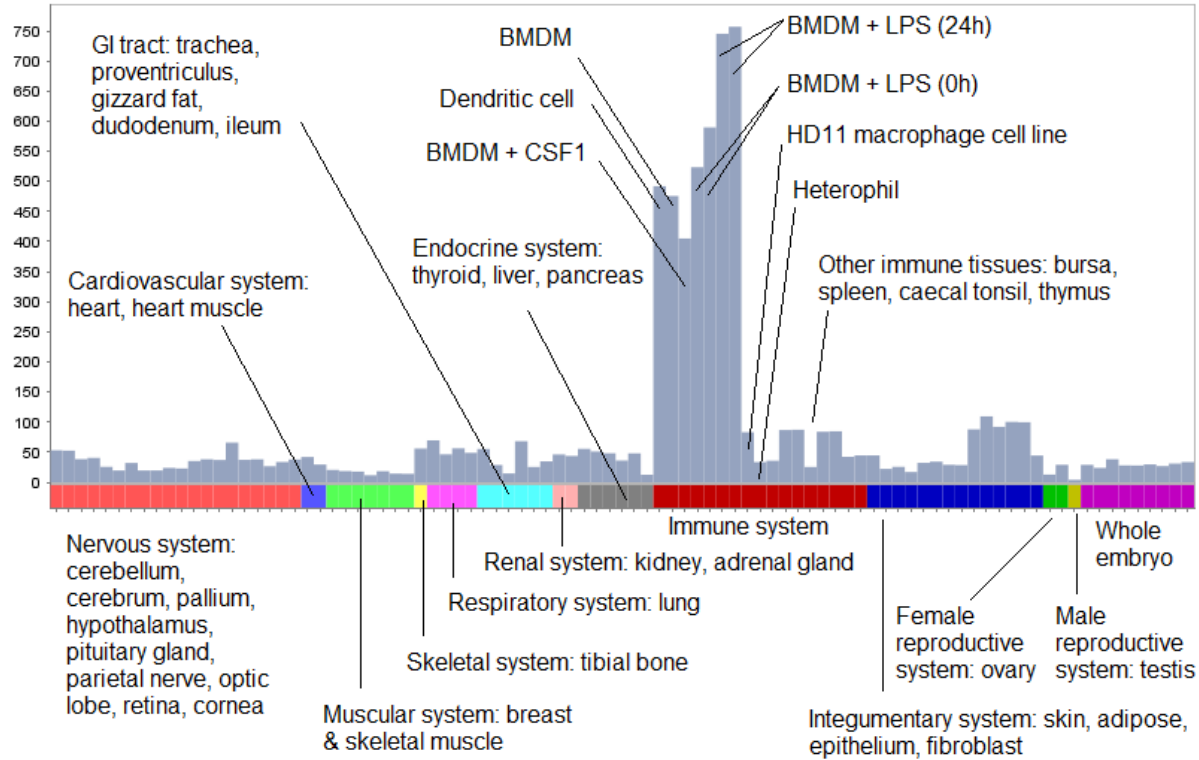
1237  
1238 **Figure 2.** Randomly down-sampling RNA-seq reads has minimal impact on the overall expression  
1239 profile, primarily affecting expression level estimates of lowly expressed genes. Data shown is from  
1240 one dataset – unchallenged BMDMs from an adult female broiler (Ross 308) – although with  
1241 quantitatively similar findings from other samples. The figure plots the average TPM per gene, taken  
1242 after 100 random samples of 10 million reads, against the TPM obtained in each sample. The line  $y = x$   
1243 is shown in red.



1244

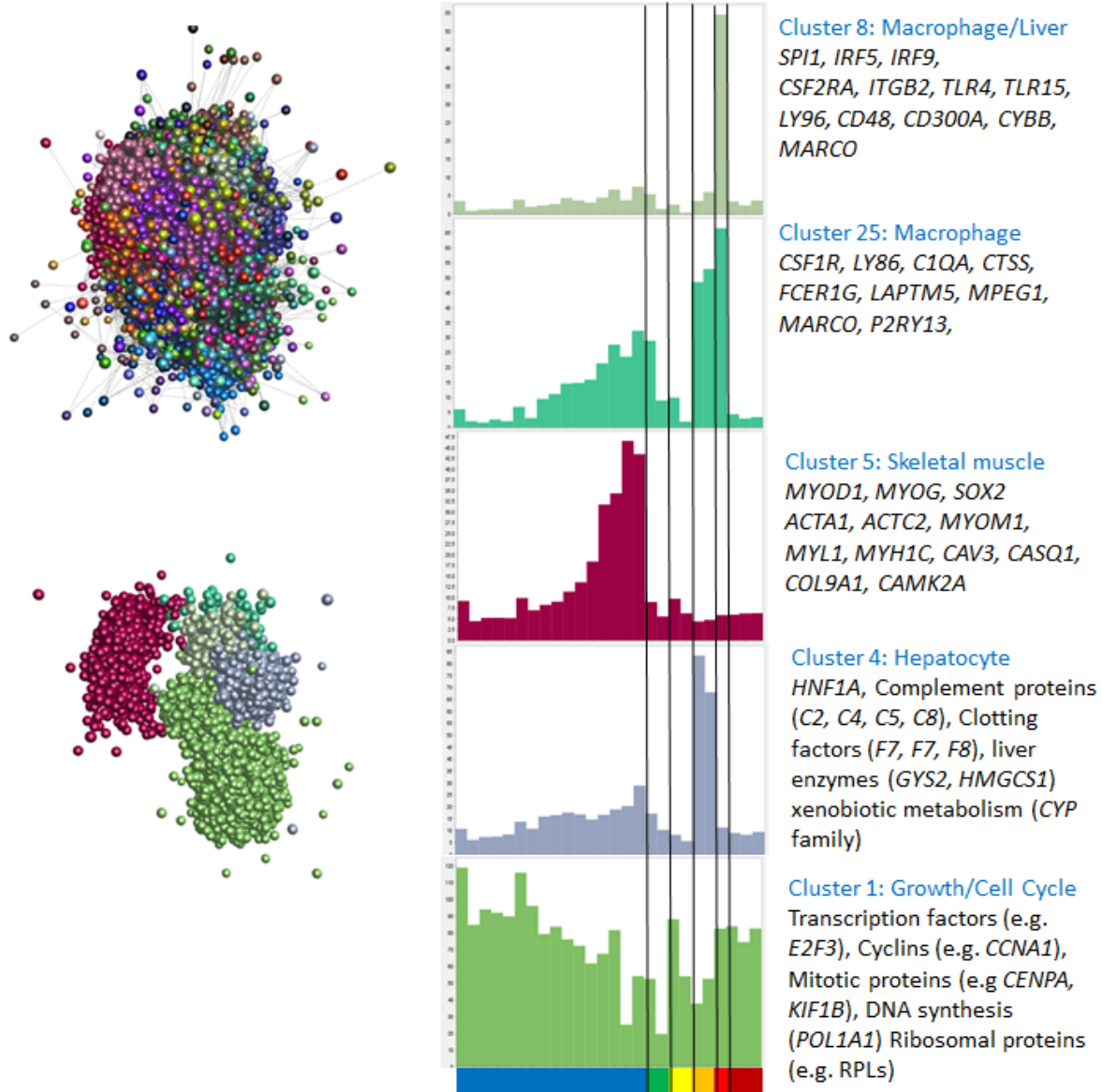
1245 **Figure 3.** 2D representation of a sample-to-sample network graph, plotting Spearman's correlations  
1246 between expression profiles. The graph was built using an RNA-seq meta-dataset with each sample  
1247 distinct by tissue, developmental stage and BioProject of origin, and expression level per gene per  
1248 sample averaged (where possible) across all replicates of that sample (dataset available as Table S6).  
1249 Each node (circle) in the graph represents a sample, and each edge (line) a correlation exceeding a  
1250 threshold ( $\rho \geq 0.82$ ). The graph contains 82 nodes, connected by 243 edges. Selected nodes are  
1251 labelled. Overall, like tissues tend to correlate more strongly with like, irrespective of BioProject of  
1252 origin. Certain coloured nodes indicate tissues independently sequenced by multiple BioProjects  
1253 (listed in Table S2), including liver (red), spleen (yellow), lung (orange), adipose (pink), caecal tonsil  
1254 (light blue) and muscle (green). There are two notable idiosyncrasies: one of the four lung samples is

1255 comparatively dissimilar to the others of its group, as is one of the three caecal tonsil samples. In the  
1256 latter case, however, the two most closely correlated caecal tonsil samples are those infected with  
1257 *Campylobacter*. Consistent with this, these samples cluster more closely with immune cells and  
1258 tissues. The third caecal tonsil sample belongs to a healthy chicken.



1259  
1260 **Figure 4.** Expression profile of the macrophage-specific cluster 4. Histogram shows the average  
1261 expression level of the 458 genes in the cluster, where expression level per gene is calculated as the  
1262 median TPM across all replicates, per BioProject, per tissue. The expression level dataset is available  
1263 as Table S6.

1264



1265

1266 **Figure 5.** The panel on the left shows the clustered nodes for the main element in the layout graph  
1267 (upper section). Nodes allocated to the same cluster are the same colour. The panel on the right shows  
1268 the average expression profiles for five clusters highlighting the different phases of chick embryo  
1269 development, and key genes for each cluster are shown in the boxes. The layout of these clusters  
1270 within the main element is shown in the lower part of the left panel. Node colour matches the colour of  
1271 the bars on the histograms. The X-axis shows the different samples (blue – embryo developmental  
1272 time course from 1.5 hours to day 20 after fertilisation (HH45); green – extraembryonic tissues;  
1273 yellow – limb buds; orange – hepatocytes; red – bone marrow derived mesenchymal stem cells; dark

1274 red – aortic smooth muscle cells. Full detail of the samples can be found in Lizio, *et al.* [53]. Y axis  
1275 shows average TPM for TSS in the cluster for each sample.  
1276



1277  
1278 **Figure 6.** ZENBU (<http://fantom.gsc.riken.jp/zenbu/>) view of the chicken *CSF1R* locus, identifying  
1279 the transcription start site downstream of the *PDGFRB* locus (A), and the time course of appearance of  
1280 *CSF1R* transcripts in the embryo and their expression in isolated cells (B).

1281

1282 **TABLES**1283 **Table 1.** Genes in cluster 14 with known function.

Gene symbol	Gene name	Protein function	References
AMZ1	archaemetzincin 1	metalloprotease, possibly involved in tissue remodelling to form feather follicles	[140, 141]
ANKK1 (PKK2)	ankyrin repeat and kinase domain containing 1	interacts with keratin filaments	[142]
AREG	amphiregulin	epithelial growth factor	[143]
CLDN9	claudin 9	tight junction membrane protein found in all epithelia	[144]
DLX4	homeobox protein DLX4	homeobox protein that regulates epithelial-mesenchymal interactions	[145]
EDMTF4  EDMTFH	epidermal differentiation protein starting with MTF motif 4  epidermal differentiation protein starting with MTF and rich in histidine	markers of the feather barbule and members of the epidermal differentiation complex; this has a role in integumentary development, including feather pigmentation	[146-148]
FK21	feather keratin 21	feather keratins	

FK27	feather keratin 27		
PNPLA4	patatin-like phospholipase domain-containing protein 4	enzyme with a role in retinol metabolism (retinol and related compounds regulate epithelial cell growth and differentiation)	[149, 150]
RAB38	Ras-related protein RAB38	GTPase involved in melanosome biogenesis and epithelial pigmentation	[151, 152]
RASSF10	Ras association domain family member 10	tumour suppressor that mediates the epithelial-mesenchymal transition	[153]
SDR16C5 (RDH-E2)	epidermal retinol dehydrogenase 2	overexpressed in psoriatic human skin	[154]
XG	Xg blood group	blood group antigen	[155]

1284 **SUPPLEMENTAL MATERIAL**

1285

1286 Dataset S1. Expression level estimates generated after randomly down-sampling the BMDM (+/- LPS)  
1287 datasets to 10 million reads 100 times.

1288

1289 Table S1. Data sources for creating an RNA-seq meta-atlas.

1290 Table S2. Independent datasets sequencing the same tissue/cell type.

1291 Table S3. Exponents of the log-log plots after plotting the reverse cumulative distribution of TPM per  
1292 gene on a log-log scale.

1293 Table S4. Number of genes with detectable expression, per tissue, after the first iteration of Kallisto.

1294 Table S5. Transcripts not detectably expressed (at > 1 TPM) in any tissue, after the first iteration of  
1295 Kallisto.

1296 Table S6. Chicken RNA-seq meta-dataset, after the second (and final) iteration of Kallisto.

1297 Table S7. Proportion of RNA-seq reads retained by down-sampling the LPS-stimulated BMDM  
1298 datasets.

1299 Table S8. Number of detectably expressed genes after randomly down-sampling the LPS-stimulated  
1300 BMDM datasets.

1301 Table S9. Range of expression estimates, and absolute difference between largest and smallest  
1302 estimate, after randomly down-sampling the LPS-stimulated BMDM datasets.

1303 Table S10. GO term enrichment for those subsets of genes whose highest PEM is for a given tissue.

1304 Table S11. All-against-all correlation matrix for each tissue in the meta-dataset.

1305 Table S12. Tissues whose expression vectors are most strongly correlated with each other.

1306 Table S13. Clusters of co-expressed genes (obtained via network analysis of the RNA-seq meta-  
1307 dataset), including candidate gene names for unannotated GalGal5 protein-coding genes.

1308 Table S14. Proportion of genes in each co-expression cluster whose highest PEM is for a given tissue.

1309 Table S15. GO term enrichment for co-expression clusters containing  $\geq 100$  genes.

1310 Table S16. Correlation of expression profiles for genes with a known protein-protein interaction.

1311 Table S17. Clusters of co-expressed CAGE tags, obtained via network analysis of the Lizio, *et al.*

1312 dataset [53].

1313 Table S18. Comparison of co-expression clusters between the RNA-seq atlas and the Lizio, *et al.*

1314 CAGE dataset [53].